

1 We thank the reviewer for their thoughtful comments and address each one below (shown in
2 red).

3 Interactive comment on “Warm Winter, Thin Ice?” by Julienne Stroeve et al. Anonymous
4 Referee #1 Received and published: 3 February 2018 Warm Winter, Thin Ice by Stroeve and
5 others

6
7 Summary: Stroeve and others investigate the impact of 2016/2017 anomalously warm winter on
8 sea ice thickness using the CICE model and CS2 thickness observations. A secondary objective
9 of the study is to compare three difference approaches of ice thickness retrievals from CS2 to
10 CICE. The authors demonstrate that recent warm fall temperatures (i.e. since 2012) impact
11 winter sea ice thickness by reducing wintertime growth which was particularly strong in
12 2016/2017. Overall, I think this manuscript can find a place in the literature when the author’s
13 address my major concern that thinning in 2016/2017 especially, north of Greenland and the
14 Canadian Archipelago was not entirely driven by thermodynamics (i.e. positive snow depth
15 anomalies) but rather reduced ice convergence.

16 **We thank the reviewer for their comment. We agree with the reviewer that the anomaly in**
17 **2016/2017 was not entirely driven by thermodynamics and thus it is a fair point that we**
18 **should have discussed in more detail. In response we have now stated more explicitly the**
19 **role that dynamics also played in reducing the ice thickness north of CAA. We actually**
20 **already showed this in our model results (strong negative dynamical thickness reduction**
21 **for 2017 in Figure 4 from CICE and also the free-CICE simulation as well as by the ice**
22 **motions in Figure 8. Thus, we have now made this point clearer in our discussion of the**
23 **results. We appreciate the reviewer pointing out our need to expand on this discussion.**

24
25
26 Major comment: The authors have not made a convincing argument that snow depth is the
27 primary mechanism for reduced ice thickness north of Greenland and the Canadian Archipelago
28 in April 2017. While I agree snow depth is the major source of uncertainty in CS2 retrievals, ice
29 dynamics during the winter of 2017 in this region was likely more influential and should be
30 discussed.

31 **See our comments above.**

32
33
34 The authors suggest the positive ice thickness anomaly in November 2016 north of Greenland
35 and the Canadian Archipelago did not persist because of snow loading and in turn reduced
36 thermodynamic growth but ice dynamics (i.e. lack of ice convergence) is more likely the culprit
37 here. Indeed, the fall of 2016 was the warmest on record and these temperature anomalies
38 persisted into 2017, thinning ice in some regions (Barents Sea) but this thinning also manifested
39 enhanced surface heating changing atmospheric circulation over the Arctic and especially over
40 the Beaufort Sea. Consequently, the Beaufort High collapsed in the winter of 2017 and this
41 reduced ice convergence against the northern Canadian Archipelago and Greenland which is
42 clearly apparent from the sea ice motion vectors in Figure 8 of the author’s paper. The latter
43 process seems to be more likely the cause of why the November ice thickness anomaly in this
44 region was not preserved as atmospheric circulation prevented dynamic ice growth
45 (convergence) which typically dominates during the winter in this region. I think the authors

Formatted: Right: 0.25"

1

46 should acknowledge that ice thinning in the Arctic is not entirely thermodynamically driven and
47 ice dynamics also play a role which is underscored by Kwok, 2015, GRL.

48
49

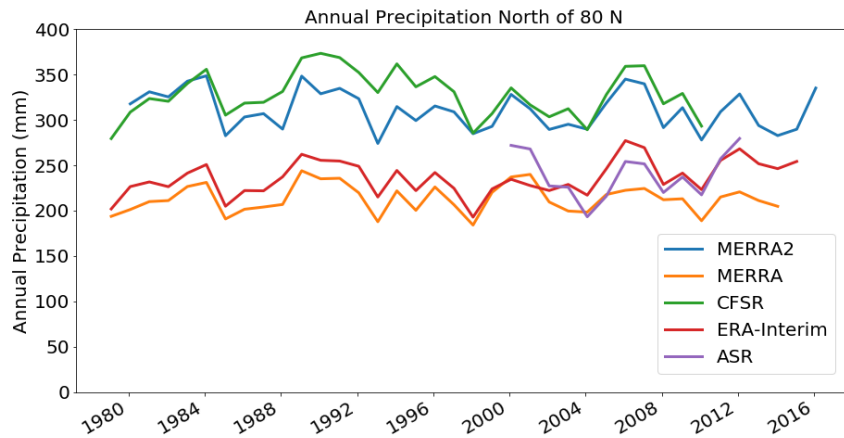
50 **We agree with the reviewer (as noted in our comments above) and we have discussed this**
51 **more extensively in the revised version.**

52

53 A second related point is that multi-year ice is the dominant ice type north of Greenland and the
54 Canadian Archipelago which has consistently been preserved despite the shift from multi-year
55 ice to first-year ice elsewhere in the Arctic. This suggests that the snow depth here should be
56 somewhat similar to the Warren Climatology. This was actually reported to be the case based on
57 recent measurements from Haas et al., 2017, GRL and hence CS2 estimates in this thick MYI
58 region should be reliable.

59

60 **While I was a co-author on the Haas et al. paper, I disagree with the assertion that we**
61 **should expect each year the snow depth to be on the same order as climatology. Snow depth**
62 **varies considerably from year to year. In fact, we find in the reanalysis data used in the**
63 **CICE simulations that there are years with anomalously high and low snow accumulation**
64 **which is illustrated in Figure 10. Regions with the largest standard deviation are actually**
65 **north of the CAA. In addition, the figure below shows the interannual variability of Arctic**
66 **precipitation from 5 different reanalysis, which clearly shows large interannual variability.**
67 **Thus, we cannot conclude that snow depth anomalies do not play a role in year-to-year sea**
68 **ice thickness variability in the currently processed CS2 data products.**



69
70
71
72
73
74

The latter point also lends further support to reduced ice convergence being more influential on thinning than thermodynamics.

Formatted: Right: 0.25"

75 Specific Comments

- 76 1. Line 286-288 Ok, but there appears to be a mix of positive and negative anomalies. The
77 most prominent feature worth mentioning is the CS2 strongest thinning anomalies are
78 along the northern coast of the Canadian Archipelago.

79 **Made changes as suggested by the reviewer. Below is the new paragraph:**

80 *Focusing more on April 2017, the 3 CS2 products suggest widespread thinner ice in April*
81 *2017 north of Ellesmere Island (up to -80 cm thinner) relative to the 2011-2017 mean*
82 *[Figure 4(top)]. Thinner ice is also found within the Chukchi and East Siberian seas (on*
83 *average -10 to -35 cm thinner) despite a mix of positive and negative anomalies. CICE*
84 *simulations on the other hand show more widespread thinning throughout the western Arctic,*
85 *including the Beaufort Sea and positive thickness anomalies north of Ellesmere Island*
86 *[Figure 4(middle and bottom)]. In the Beaufort Sea, there is general disagreement among*
87 *the 3 CS2 products and the CICE simulations: regional mean anomaly of -5 cm (CPOM), 0*
88 *cm (AWI), +20 cm (NASA), -25 cm (CICE-ini) and -30 cm (CICE-free). North of Ellesmere*
89 *Island, CICE-ini indicates positive thickness anomalies (up to +50 cm), whereas all 3 CS2*
90 *products show negative thickness anomalies (up to -80 cm). In this region, the CICE-free*
91 *simulation also shows mostly negative thickness anomalies (-20 to -80 cm), with a small*
92 *positive area (up to +25 cm).*

- 93
94
95 2. Line 297-299 I'm not convinced that the snow loading in CS2 has caused this difference
96 in April 2017 north of the Canadian Archipelago and Greenland. If I recall, the Beaufort
97 High collapsed in the winter of 2017 and this reduced convergence against the northern
98 Canadian Archipelago and Greenland which appears to the case in Figure 8. The latter
99 seems more likely the cause of why the thickness anomaly in this region was not
100 preserved as atmospheric circulation prevent dynamic ice growth. This seems to be
101 captured across all CS2 products but not CICE-ini. This needs revision. See major
102 comment.

103 **We agree. See our responses to your major comment above, and see the revisions**
104 **made between lines 316 to 343 pasted below.**

105 *On the other hand, thickness is also strongly influenced by dynamics, such as*
106 *convergence against the CAA and Greenland which leads to thicker ice in this region*
107 *[Kwok et al., 2015]. During winter 2017 however, the Beaufort High largely collapsed,*
108 *reducing convergence against the northern CAA and Greenland [Figure 8]. One*
109 *advantage of using CICE, is that we can more readily diagnose thermodynamic vs.*
110 *dynamical contributions to the observed thickness anomalies. For the region directly*
111 *north of Ellesmere Island, both the CICE-ini and CICE-free simulations support reduced*
112 *sea ice convergence, leading to thinner ice from dynamical contributions. At the same*
113 *time, this region also exhibited reduced thermodynamic ice growth in both CICE*
114 *simulations. One would expect thermodynamic ice growth to be reduced in regions of*
115 *enhanced snow depth and thicker November ice. Positive snow depth anomalies extended*
116 *from this region through the northern Beaufort Sea, in agreement with extended regions*
117 *reductions in thermodynamic ice growth in both CICE-free and CICE-ini. At the same*
118 *time, regions of positive 2016 November thickness anomalies are also associated with*
119 *regions of reduced CICE thermodynamic ice growth.*

Formatted: Right: 0.25"

120 3. Line 413-415 The snow is important but ice thickness is strongly influence by dynamics
121 (i.e. convergence against the Canadian Archipelago and Greenland) and this needs to be
122 mentioned in the discussion as well. See Kwok, 2015, GRL. Furthermore, MYI is the
123 dominant ice type north of Greenland and the Canadian Archipelago which has
124 consistently been preserved despite the shift from MYI to FYI elsewhere. This suggests
125 the snow depth here should be similar to the W99 which was found reported by Haas et
126 al., 2017, GRL hence CS2 estimates here should be reliable and lends further support to
127 reduced ice convergence was more influential on thinning. See major comment.

128 **See our responses to your major comment above.**

129
130 4. Table 1 What is the source of the data in this table? The passive microwave algorithm
131 from Markus et al., 2009, JGR?

132 **Yes, from Markus et al. 2009 and from Stroeve et al., 2014. References were**
133 **mentioned in the body text, but now also added to the Table caption.**

134 5. References: Haas, C., Beckers, J., King, J., Silis, A., Stroeve, J., Wilkinson, J.,
135 Notenboom, B., Schweiger, A., & Hendricks, S. (2017). Ice and snow thickness
136 variability and change in the high Arctic Ocean observed by in situ measurements.
137 Geophysical Research Letters, 44, 10,462–10,469.
138 <https://doi.org/10.1002/2017GL075434> Kwok, R. (2015), Sea ice convergence along the
139 Arctic coasts of Greenland and the Canadian Arctic Archipelago: Variability and
140 extremes (1992–2014), Geophys. Res. Lett., 42, 7598–7605,
141 doi:10.1002/2015GL065462.

142 **Thank you, these have been added.**

143
144
145
146
147
148
149
150
151
152
153
154
155
156
157
158
159
160
161
162
163
164

Formatted: Right: 0.25"

165 Review for "Warm Winter, Thin Ice?" by Stroeve et al.
166 **We thank the reviewer for their thoughtful comments and our responses are shown in red**
167 **below.**

168 Summary

169 This paper uses model simulations from the Los Alamos sea-ice model (CICE) and
170 CryoSat-2 thickness estimates from three different data providers to investigate the
171 impact of the 2016/2017 anomalously warm winter on Arctic sea ice thickness. The
172 authors consider free CICE simulations as well as CICE simulations initialized with
173 CryoSat. Coinciding with the least amount of freezing degree days north of 70N since
174 1979, the authors find that CICE simulations in April 2017 show the thinnest ice cover
175 in the Arctic Basin over the CryoSat-2 data period. However, this finding is not entirely
176 supported by the satellite retrievals. CICE simulations are also used to investigate the
177 processes leading to ice thickness anomalies, separating dynamic and thermodynamic
178 contributions. It is concluded that free CICE simulations from 1985 to 2017 reveal that
179 the correlation between winter ice growth and November ice thickness is stronger than
180 between growth and FDDs, although this correlations has become weaker since 2012,
181 and delayed freeze up due to warmer winter temperatures play a bigger role.

182
183 General comments:

184 The impact of warmer winter seasons on the Arctic ice cover is of high interest for
185 the sea ice and climate science community. In addition, the comparison between sea
186 ice thickness retrievals from different providers adds some valuable information here.
187 The manuscript itself is well written, but there are lots of information in the figures
188 and tables which are not easy to capture. For example, color bars in Figure 4 show
189 different scales, which is a bit confusing. Also the quality of the figures in general can
190 be improved. See more detailed comments below.

191 Apart from that, my major concern is that it is **not really well explained how reliable**
192 **the model simulations are**, both CICE free and CICE initialized with CryoSat. Although
193 the mean monthly values seem to fit quite well to the satellite observations, considering
194 Figure 3 and Figure 5, **regional anomalies disagree quite significant in several**
195 **cases**. For example, the significant positive thickness anomaly north of the Canadian
196 Archipelago in April 2014 and 2015 is rather weak in the model simulations. I don't
197 think that this is due to the usage of a snow climatology in the satellite retrievals, since
198 this area is mostly covered by multiyear sea ice. I also wonder why this strong positive
199 anomaly is not present at least in the CICE simulations initialized with CryoSat. Based
200 on these concerns, I also wonder **how reliable the findings and conclusions regarding**
201 **the results presented in Figure 9** are. Could you include the satellite observations here
202 as well? Also difference maps and scatter plots between simulated ice thicknesses and
203 CryoSat ice thicknesses would be interesting and could potentially help to support the
204 conclusions and show more explicit the limitations of the model simulations. For example,
205 how meaningful are the correlations given in the maps of Figure 9 if the model is
206 limited in reproducing regional anomalies as described above?

207

Formatted: Right: 0.25"

5

208 Local and to a lesser extent regional results from our model simulations are affected by a
209 variety of uncertainties, including slightly shifted location of moving cyclones can result in
210 wrong pattern of ice drift and ice divergence, and reanalysis precipitation likely has biases as
211 well. Thus, we do not believe, nor do we state that all the small regional features shown in the
212 maps in Fig. 4 to 6 are realistic. At this scale we are only confident for regions where CryoSat-2
213 products and CICE simulations agree (see original paragraphs lines 263-285). In Figure 9,
214 however, we are looking at an Arctic Basin wide mean. For the Arctic Basin wide mean,
215 thermodynamic processes are dominating over the dynamic processes (see Table 3) and the
216 thermodynamic winter ice growth has been tuned successfully to agree with the Cryosat winter
217 ice growth. Thus, our results on this scale are reliable as further demonstrated by Fig. 1b. There
218 are no satellite observations of ice thickness available which cover a period of more than 30
219 years and thus, it would not be correct to use those for Figure 9 as the time-period is simply too
220 short for meaningful correlations. We have added a comment on lines 268-270 to highlight that
221 fact up front (*While we discuss some of the regional differences below, we are most confident in
222 the model simulations on the Arctic Basin-wide scale over which CICE has been tuned to agree
223 with CS2 winter ice growth.*).

224
225 In response to the comments on the plots and color bars, we have made improvements that
226 hopefully satisfy the reviewers concerns.

227
228 Detailed comments:

229 P3 L109: The CPOM product is derived using a 70 % threshold, not 50 % as stated
230 in this paper (and in Laxon et al. (2013) because of a typo). There is an erratum for
231 Laxon et al. (2013) where a 70% threshold is reported.

232 Thank you for pointing this out, it has now been corrected.

233
234 P3 L124: Category 1 ranges up to 0.6 m. But when you discard any measurements
235 below 0.5 m, then you this category only covers a very narrow range of thickness. Isn't
236 that a limitation for the initialization of the model then?

237 We discard grid point with a mean thickness below 0.5m, but otherwise we include all
238 individual measurements. We state that "Grid points with less than 100 individual
239 measurements and a mean SIT < 0.5 m are not included." But have now added the extra
240 statement to avoid confusion: "Otherwise, all individual observations are included"

241
242 P3 L138: CICE simulations - What are the grid cell ice thicknesses in the CICE simulations
243 representing? The mean thickness of the ice covered area or the mean thickness
244 of the entire area including open water? This information should be given in this section,
245 because it is crucial when comparing it with the satellite data.

246 This is a good point. We have now added at the end of this section the statement: "For
247 comparison with CS2 we present the mean thickness of the ice covered area. In winter the sea
248 ice concentration in the model is generally between 0.98 and 0.995% apart from locations close
249 to the ice edge".

250
251 Figure 1 c): Information about the red and the yellow areas is missing.

Formatted: Right: 0.25"

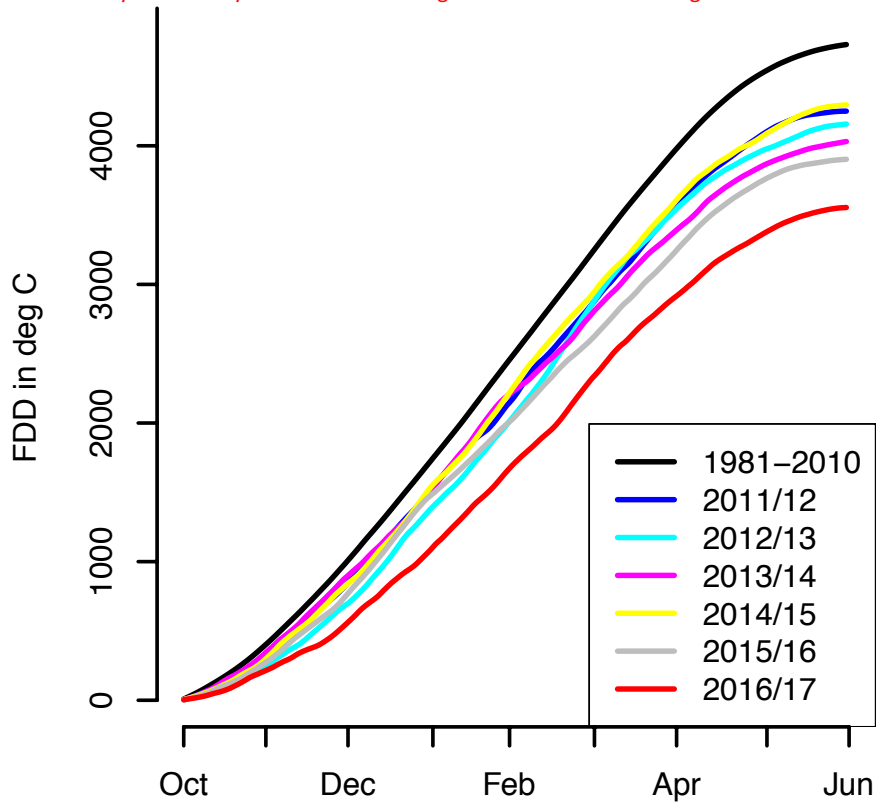
252 Corrected.

253

254 Figure 2, L677: I cannot see any light gray areas. The legend in Fig 2c is very small.

255 We have increased the size of the legend. We removed the statement about the light gray

256 areas as they are actually shown in white in Figure 2d. Here is the new Figure 2c.



257

258 Figures 3, 5, 6, 11: The labels of the color tables are too small. Since all maps of each
259 figure correspond on the same thickness range, I suggest to use just one color bar and
260 make it bigger.

261 We have removed the individual color bars and now just use one larger horizontal color bar.

262

263 Figure 4: It is a bit confusing that you use different thickness ranges for the CICE

264 anomaly contributions from thermodynamics and dynamics (+/- 0.4), while for the other

265 maps, you use +/- 0.8. I suggest to use a uniform range, e.g. +/- 0.8. This would make

Formatted: Right: 0.25"

266 a comparison with the other maps easier.
267 We agree and made the suggested change.
268

269 Second, I wonder how to interpret the thermodynamic and dynamic contributions. For
270 example, there is a positive CICE anomaly north of the archipelago (middle left), while
271 both the thermodynamic (middle center) and dynamic (middle right) contributions show
272 negative anomalies. How is this explained?

273 Well, in your example a very strong positive CICE anomaly in Nov 2016 (Fig. 3) has been
274 reduced by thermodynamic and dynamic processes (positive anomalies) to result in a weaker,
275 but still positive anomaly in April 2017. Thus, the initial conditions in November are responsible.
276 Thermodynamic contribution consists of local ice growth/melt and dynamic contribution of
277 advection and ridging processes during the period November to the following April.
278

279 Moreover, there is a typo in the caption (L692). I suppose contribution of dynamics is
280 shown in the "right" column.

281 Yes, thank you.
282

283
284
285

286 Warm Winter, Thin Ice?

287 Julienne Stroeve^{1,2}, David Schroder³, Michel Tsamados¹, Daniel Feltham³

288
289 ¹Centre for Polar Observation and Modelling, Earth Sciences, University College London,
290 London, UK

291 ²National Snow and Ice Data Center, University of Colorado, Boulder, CO, USA

292 ³Centre for Polar Observation and Modelling, Department of Meteorology, University of
293 Reading, Reading, UK
294

295 Abstract

296 Winter 2016/2017 saw record warmth over the Arctic Ocean, leading to the least amount of
297 freezing degree days north of 70°N since at least 1979. The impact of this warmth was evaluated
298 using model simulations from the Los Alamos sea-ice model (CICE) and CryoSat-2 thickness
299 estimates from three different data providers. While CICE simulations show a broad region of
300 anomalously thin ice in April 2017 relative to the 2011-2017 mean, analysis of three CryoSat-2
301 products show more limited regions with thin ice and do not always agree with each other, both
302 in magnitude and direction of thickness anomalies. CICE is further used to diagnose feedback
303 processes driving the observed anomalies, showing 11-13 cm reduced thermodynamic ice growth
304 over the Arctic domain used in this study compared to the 2011-2017 mean, and dynamical
305 contributions of +1 to +4 cm. Finally, CICE model simulations from 1985-2017 indicate the
306 negative feedback relationship between ice growth and winter air temperatures may be starting to
307 weaken, showing decreased winter ice growth since 2012 as winter air temperatures have
308 increased and the freeze-up has been further delayed.
309

310 Introduction

Formatted: Right: 0.25"

311 It is well known that Arctic air temperatures are rising faster than the global average [e.g.
312 *Bekryaev et al.*, 2010; *Serreze and Barry*, 2011]. The thinning and shrinking of the summer sea
313 ice cover have played a role in this amplified warming, which is most prominent during the
314 autumn and winter months as the heat gained by the ocean mixed layer during ice-free summer
315 periods is released back to the atmosphere during ice formation [e.g. *Serreze et al.*, 2009; *Screen*
316 *and Simmonds*, 2010]. However, Arctic amplification has been found in climate models without
317 changes in the sea ice cover [*Pithan and Mauritsen*, 2014]. Increased latent energy transport
318 [*Graversen and Burtu*, 2016], the lapse rate feedback [*Pithan and Mauritsen*, 2014; *Graversen*,
319 2006] and changes in ocean circulation [*Polyakov et al.*, 2005] have also contributed.
320 Furthermore, cyclones are effective means of bringing warm and moist air into the Arctic during
321 winter [e.g. *Boisvert et al.*, 2016].

322 Winter 2015/2016 was previously reported as the warmest Arctic winter recorded since
323 records began in 1950 [*Cullather et al.*, 2016]. Warming was Arctic-wide, with temperature
324 anomalies reaching +5°C [*Overland and Wang*, 2016] and temperatures near the North Pole
325 hitting 0°C [*Boisvert et al.*, 2016]. Part of the unusual warming was linked to a strong cyclone
326 that entered the Arctic in December 2015 [*Boisvert et al.*, 2016], resulting in reduced
327 thermodynamic ice growth and thinning within the Kara and Barents seas [*Ricker et al.*, 2017;
328 *Boisvert et al.*, 2016]. This was one of several cyclones to enter the Arctic that winter as a result
329 of a split tropospheric vortex that brought warm and moist air from the Atlantic Ocean towards
330 the pole [*Overland and Wang*, 2016]. Winter 2016/2017 once again saw temperatures near the
331 North Pole reach 0°C in December 2016 and February 2017 [*Graham et al.*, 2017]. These
332 warming events were similarly associated with large storms entering the Arctic [*Cohen et al.*,
333 2017]. It has been suggested that the recent warm winters represent a trend towards increased
334 duration and intensity of winter warming events within the central Arctic [*Graham et al.*, 2017].

335 In general, warm winters, combined with increased ocean mixed layer temperatures from
336 summer sea ice loss, delay freeze-up, impacting the length of the ice growth season and the
337 period for snow accumulation on the sea ice. *Stroeve et al.* [2014] previously evaluated changes
338 in the melt onset and freeze-up, showing large delays in freeze-up within the Chukchi, East
339 Siberian, Laptev and Barents seas, with delays increasing on the order of +10 days per decade.
340 Later freeze-up has a non-trivial influence on basin-wide sea ice thickness: ice grows
341 thermodynamically faster for thin ice than for thick ice [*Bitz and Roe*, 2004]. More subtle effects
342 involving the timing of ice growth relative to major snow precipitation events in fall have been
343 shown to also control the growth rate of sea ice thickness; ice grows faster for a thinner snow
344 pack [*Merkouridi et al.*, 2017]. Nevertheless, the maximum winter sea ice extent in 2017 set a
345 new record low for the 3rd year in a row. Have the recent warm winters played a role in these
346 record low winter maxima by reducing winter ice formation?

347 *Ricker et al.* [2017a] previously evaluated the impact of the 2015/2016 warm winter on ice
348 growth using sea ice thickness derived from blending CryoSat-2 (CS2) radar altimetry with those
349 from Soil Moisture and Ocean Salinity (SMOS) radiometry [*Ricker et al.*, 2017b]. They found
350 anomalous freezing degree days (FDDs) between November 2015 and March 2016 within the
351 Barents Sea of 1000 degree days coincided with a thinning of approximately 10 cm in March
352 compared to the 6-year mean. While near-surface air temperatures largely control
353 thermodynamic ice growth, other processes also impact ice growth, including ocean circulation,
354 sensible and latent heat exchanges. Furthermore, winter ice thickness is not only a result of
355 thermodynamic ice growth, but rather the combined effects of thermodynamic and dynamic
356 processes. A thinner ice cover is more prone to ridging and rafting, as well as ice divergence,

Formatted: Right: 0.25"

357 leading to new ice formation within leads/cracks within the ice pack. This however was not
358 evaluated by *Ricker et al.* [2017a].

359 In this study we evaluate the impact of the 2016/2017 anomalously warm winter on Arctic
360 sea ice thickness using the Los Alamos sea-ice model (CICE) [*Hunke et al.*, 2015] and satellite-
361 derived CS2 thickness data from three different sources: Centre for Polar Observation and
362 Modeling (CPOM) [*Tilling et al.*, 2017], Alfred Wegener Institute (AWI) [*Hendricks et al.*,
363 2016], and NASA [*Kurtz and Harbeck*, 2017]. CICE is initialized with CPOM CS2 sub-grid
364 scale ice thickness distribution (ITD) fields in November and run forward with NCEP
365 Reanalysis-2 (NCEP2) atmospheric reanalysis data [*Kanamitsu et al.*, 2002, updated 2017]. The
366 model run is subsequently compared over the winter growth season to CS2 thickness from the
367 three different data providers and contributions of thermodynamics vs. dynamics to the thickness
368 anomalies are evaluated. While the focus is on the 2016/2017 ice growth season, a secondary
369 aim is to compare existing CS2 products to inform the community on uncertainties in these
370 estimates and inform on model limitations. Thus, results are also presented for other years during
371 the CS2 time-period for comparison. To our knowledge, this is the first study to compare
372 different CS2 data products over the lifetime of the mission.

373 **Methods**

374 *Ice Thickness Distribution (ITD) from Cryosat-2*

375 The CryoSat-2 radar altimetry mission was launched April 2010, providing estimates of ice
376 thickness during the ice growth season. CS2 provides freeboard estimates, or the height of the ice
377 surface above the local sea surface, which when combined with information on snow depth,
378 snow density and ice density can be converted to ice thickness assuming hydrostatic equilibrium
379 [e.g. *Laxon et al.*, 2013]. Here we evaluate ice thickness fields provided by three different data
380 providers in order to assess robustness of the observed thickness anomalies. Thickness is
381 retrieved from ice freeboard by processing CS2 Level 1B data, with a footprint of 300m by
382 1700m, and assuming snow density and snow depth from the *Warren et al.* [1999] climatology
383 (hereafter *W99*), modified for the distribution of multiyear versus first-year ice (i.e. snow depth
384 is halved over first-year ice) [see *Laxon et al.*, 2013 and *Tilling et al.*, 2017 for data processing
385 details].

386 While the three data providers rely on *W99* for snow depth and density, each institution
387 processes the radar returns differently. In general, the range to the main scattering horizon of the
388 radar return is obtained using a retracker algorithm. This can be based on a threshold [e.g. *Laxon*
389 *et al.*, 2013; *Ricker et al.*, 2014; *Hendricks et al.*, 2016], or a physical retracker [*Kurtz et al.*,
390 2014]. While the CPOM and AWI products use a leading edge 70% threshold retracker, *Kurtz*
391 *and Harbeck* [2017] rely on a physical model to best fit each CryoSat-2 waveform. This will lead
392 to ice thickness differences based on different thresholds applied: *Kurtz et al.* [2014] found a 12
393 cm mean difference between using a 50% threshold and a waveform fitting method.

394 We note that several factors contribute to CS2-derived sea ice thickness uncertainties,
395 including the assumption that the radar return is from the snow/ice interface [*Willat et al.*, 2011],
396 snow depth departures from climatology and the use of fixed snow and ice densities. In this
397 study we initialize the CICE model simulations described below with the CPOM sea ice
398 thickness fields. Accuracy of the CPOM product has been evaluated in several studies,
399 suggesting mean biases between thickness observations in 2011 and 2012 of 6.6 cm when
400 compared with airborne EM data [*Laxon et al.*, 2013; *Tilling et al.*, 2015]. For April 2017, the
401

Deleted: 50

Formatted: Right: 0.25"

403 CPOM near-real-time product [Tilling et al., 2016] was used in place of the archived product,
404 with a mean thickness bias of 0.9 cm between these products.

405 In this study, individual thickness point measurements are binned into 5 CICE thickness
406 categories (1: < 0.6m, 2: 0.6-1.4m, 3: 1.4-2.6m, 4: 2.6-3.6m, 5: > 3.6m) on a rectangular 50km
407 grid for each month. The mean area fraction and mean thickness is derived for each thickness
408 category and these values are interpolated on the tripolar 1 degree CICE grid (~40km grid
409 resolution). Grid points with less than 100 individual measurements and a mean SIT < 0.5 m are
410 not included. Otherwise, all individual observations are included. For November, this effectively
411 limits the area of the Arctic to the region shown in Figure 1(c). Negative thickness values that are
412 retained in the CS2 processing to prevent statistical positive bias of the thinner ice are added to
413 category 1. The novel approach of initializing the CICE model with the full ITD rather than the
414 mean sea ice thickness provides an additional control on the repartition of the ice among
415 different thickness categories. This in turn allows a more accurate representation of ice growth
416 and ice melt processes [Tsamados et al., 2015] compared to initializing with the mean grid-cell
417 SIT and deriving the fractions for each ice category assuming a parabolic distribution. Ice growth
418 and melt strongly depend on SIT: using a real distribution can have a big impact, especially for
419 thin ice.

420 CICE Simulations

421 CICE is a dynamic-thermodynamic sea-ice model designed for inclusion within a global
422 climate model. The advantages of using CICE for this study is that we can more readily separate
423 thickness anomalies into their thermodynamic and dynamical contributions, examine inter-
424 annual variability and perform longer simulations. For this study, we performed two different
425 CICE simulations. The first is a multiyear simulation from 1985 to 2017 (referred to as CICE-
426 free). The second is a stand-alone sea-ice simulation for the pan-Arctic region starting in mid-
427 November and running until the end of April of the following year for the last 7 winter periods
428 from 2010/2011 to 2016/2017. This results in seven 1-year long simulations (referred to as
429 CICE-ini), in which the initial thickness and concentration for each of the 5 ice categories is
430 updated from the CS2 ITD using the CPOM CS2 November thickness fields. For grid points
431 without CS2 data, and for all other variables (e.g. temperature profiles, snow volume), results
432 from the free CICE simulation with the same configuration started in 1985 are applied. In this
433 way, CICE simulations cover the pan-Arctic region, but in regions where no CS2 are available,
434 we restart SIT values from the free CICE model run. While this approach would be problematic
435 in a coupled model, in a stand-alone sea ice simulation the model adjustment to the new
436 conditions is smooth and the impact of using the vertical temperature profile from the free
437 simulation only affects sea ice thickness on the order of millimeters.

438 Snow accumulation can depart strongly from the W99 climatology for individual years. Thus,
439 we make the assumption that the deviation of the mean annual cycle of snow depth over the last
440 7 years from the W99 climatology is small and assume mean winter ice growth to be determined
441 accurately from CS2, and tuned CICE-ini accordingly to match the observed CS2 mean winter
442 ice growth from the CPOM product in the central Arctic [Figure 1]. The excellent agreement for
443 both CICE-ini and CICE-free with CS2 increases the confidence of our model results. Our
444 approach therefore allows us to study inter-annual variability from 2 model configurations with
445 different sources of errors, in addition to the 3 CS2-based products.

446 For both CICE simulations, NCEP-2 provides the atmospheric forcing. We use NCEP-2 2m
447 air temperatures because they have been shown to be more realistic for the Arctic Ocean than

Deleted: While s

Deleted: ,

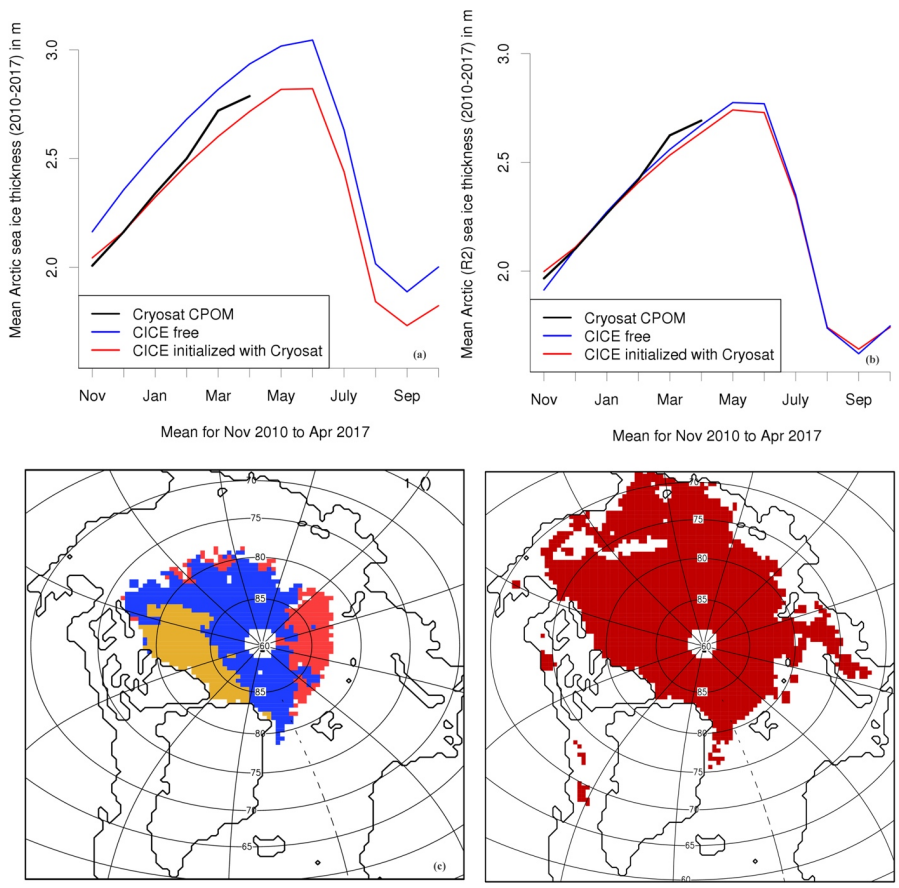
Deleted: . Thus, we

Formatted: Right: 0.25"

451 those from ERA-Interim [Jakobshavn *et al.*, 2012]. The setup is the same as described in
452 Schröder *et al.* [2014] including a simple ocean-mixed layer model, a prognostic melt pond
453 model [Flocco *et al.*, 2012] and an elastic anisotropic-plastic rheology [Tsamados *et al.*, 2013],
454 with the following improvements: we apply an updated CICE version 5.1.2 with variable
455 atmospheric and oceanic form drag parameterization [Tsamados *et al.* 2014], we increase the
456 thermal conductivity of fresh ice from 2.03 W/m/k to 2.63 W/m/K, snow from 0.3 W/m/K to 0.5
457 W/m/K and the emissivity of snow and ice from 0.95 to 0.976. While the default conductivity
458 values are at the lower end of the observed range, the new values are at the upper end and have
459 been applied in previous climate simulations [e.g. Rae *et al.*, 2014].

460 Below, all CS2-derived sea ice thickness anomalies are computed relative to the CS2 time-
461 period: November anomalies are relative to 2010-2016, and for April they are relative to 2011-
462 2017. Results for November and April are only shown for all grid cells which have a minimum
463 thickness of 50 cm and a minimum of 100 individual measurements for each of the seven years.
464 For the month of November, this corresponds to all colored area shown in Figure 1(c). For April,
465 this region represents the area in red shown in Figure 1(d). The larger region shown in Figure
466 1(d) also corresponds to the region over which the amount of thermodynamic ice growth and
467 dynamical ice growth between November and April are assessed from the CICE simulations. For
468 comparison with CS2, we present the mean thickness of the ice-covered area. In winter, the sea
469 ice concentration in the model generally ranges between 0.98 and 0.995% apart from locations
470 close to the ice edge. Further note that area-averaged values for November and April are only
471 given for regions shown in Figure 1(c) and Figure 1(d), respectively.

Formatted: Right: 0.25"



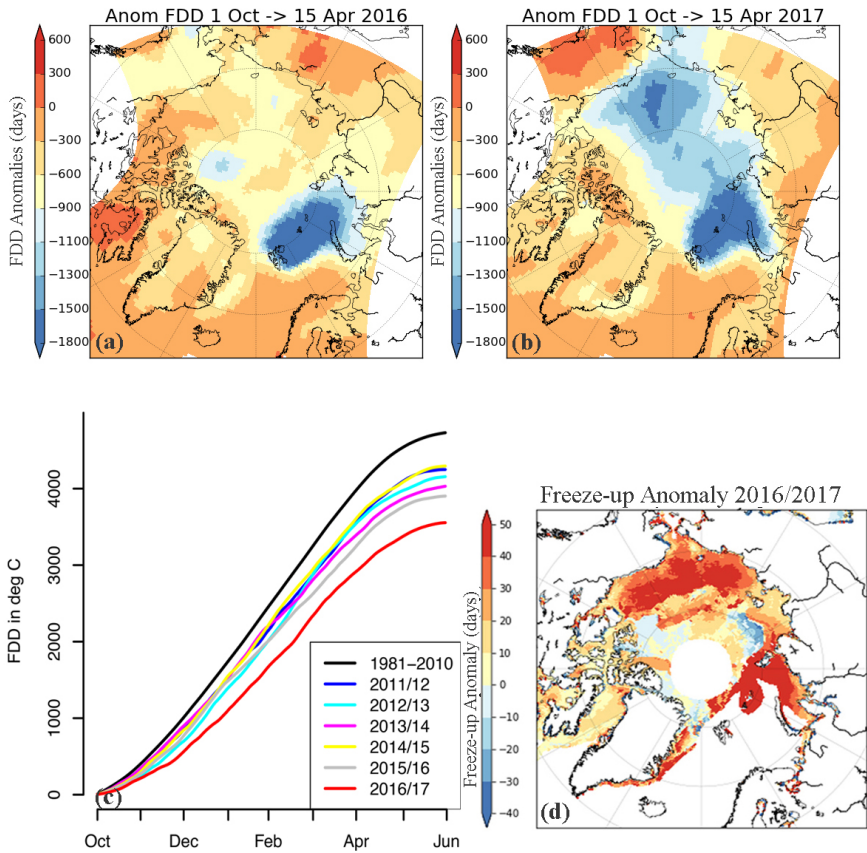
472
 473 **Figure 1.** Comparison of CPOM CryoSat-2 mean seasonal sea ice thickness (black) with CICE free (blue) and CICE
 474 initialized with Cryosat-2 in November (red). Figure 1(a) shows results for mean thickness averaged over all the
 475 colored areas shown Figure1(c), representing the total region for which Cryosat-2 data exist in November (only grid
 476 points included with > 100 measurements per month and mean thickness > 0.5m) and (b) mean thickness averaged
 477 over the sub-region shown in blue with medium thick ice in January (between 1.5 and 2.5m). Blue areas in Figure
 478 1(c) show regions between November and January where CryoSat-2 thickness are between 1.5 and 2.5 m in all
 479 years; red for thin ice (< 1.5) and orange for thick ice (> 2.5m). Figure 1(d) is the region over which the April
 480 thickness anomalies and results are presented.

481
 482 **Results**
 483 *Air temperature and freezing anomalies*

484 The growing season air temperatures anomalies (i.e. mid-November 2016 to mid-April 2017
 485 relative to 1981-2010) were positive throughout the Arctic, leading to large reductions in the
 486 number of FDDs, computed as the cumulative daily 2 m NCEP-2 air temperatures below -1.8°C,

Formatted: Right: 0.25"

487 similar to *Ricker et al.* [2016]. FDDs computed this way reflect both the number of days with air
 488 temperatures below freezing, and the magnitude of below freezing air temperatures over the
 489 specified period. Spatially, FDD anomalies show widespread reductions over most of the Arctic
 490 Ocean, with the largest reductions in the Barents and Kara seas, stretching across the pole
 491 towards the Beaufort and Chukchi seas [Figure 2b]. In contrast, during winter 2015/2016, FDDs
 492 were most notably anomalous within the Barents and Kara seas [Figure 2a], in agreement with
 493 *Ricker et al.* [2017a]. Overall, as averaged from 70-90°N, this past winter witnessed the least
 494 amount of cumulative FDDs since at least 1979 [Figure 2c].
 495



496
 497 **Figure 2.** Top panel shows the freezing degree anomalies (FDD) computed as the number of days with NCEP2 2m
 498 air temperature below -1.8°C from mid-November to mid-April in winter 2016 (a) and winter 2017 (b) computed
 499 relative to the 1981-2010 climatology. Bottom left image shows the cumulative freezing degree days (FDDs)
 500 averaged over region shown in Figure 3 inset (c), and bottom right image shows freeze-up anomalies for 2016/2017
 501 relative to 1981-2010 (d). Areas in white are either missing (pole hole) or no sea ice in winter 2016/2017.

Formatted: Font:Bold, Italic

Formatted: Right: 0.25"

502 While ice forms quickly within the central Arctic once air temperatures drop below freezing, this
503 year saw large delays in freeze-up throughout the Arctic. Updating results previously reported in
504 *Stroeve et al.* [2014], freeze-up was delayed by 20 days for the Arctic as a whole, with regions
505 like the Bering, Beaufort, Chukchi, East Siberian and Kara seas delayed by three to four weeks
506 [Figure 2d]. Within the Barents Sea, the regionally averaged freeze-up was delayed by 60 days.
507 In recent years, the trend towards later freeze-up has increased, with the Barents and Chukchi
508 seas showing the largest trends on the order of +14 days per decade through 2017, followed by
509 the Kara and East Siberian seas with delays on the order of +10 to +12 days per decade. Within
510 the Beaufort Sea, freeze-up is now happening later by +9 days per decade [Table 1].
511

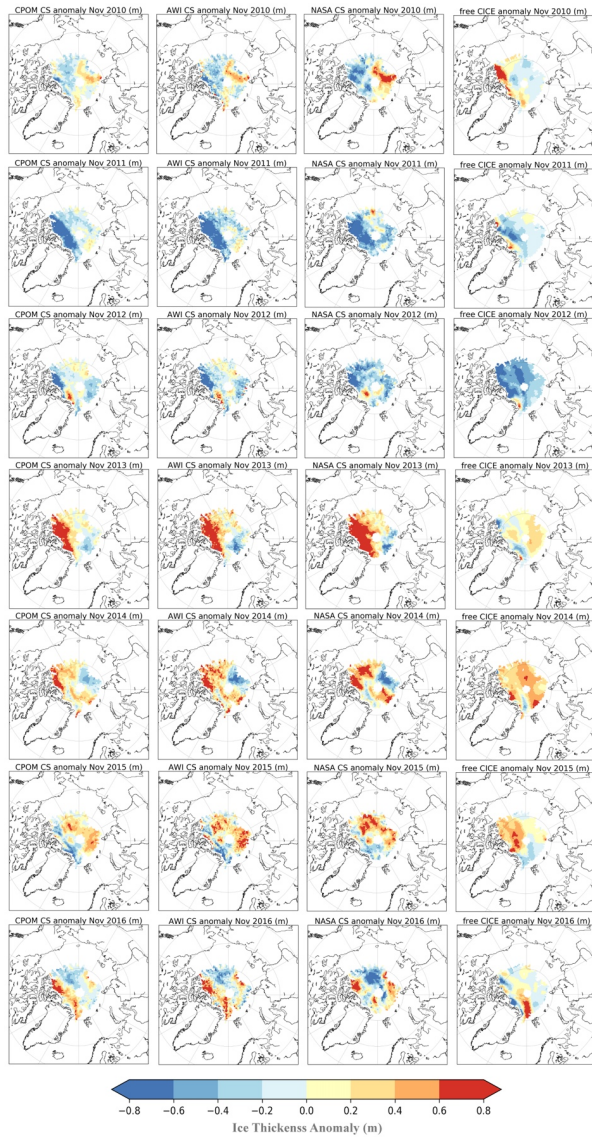
512 *November ice thickness anomalies*

513 Before analyzing how the reduced number of freezing degree days impacted winter ice
514 growth during 2016/2017, it is useful to first inter-compare the different CryoSat-2 thickness
515 estimates. We start with a comparison of November thickness from the three CS2 data sets from
516 November 2010 to 2016 [Figure 3]. It is encouraging to find that year-to-year variability in the
517 spatial patterns of positive and negative thickness anomalies are generally consistent between the
518 three products despite differences in waveform processing. The AWI and CPOM data sets are in
519 better agreement with each other than with the NASA product, which is expected as they use a
520 similar retracker. Furthermore, all three data sets show widespread thinner ice in November
521 2011, and widespread thicker ice in November 2013. This is further supported by analysis of
522 regional mean thickness and anomalies computed over the region shown in Figure 1(c) [Table
523 2]. For comparison, we also list results from the CICE-free model simulation. In November
524 2011, the different CS2 data products are in agreement that the ice was anomalously thin (-32 to
525 -46 cm), the thinnest in the CS2 data record. Similarly, in November 2013, all three CS2
526 products show overall thicker ice on the order of +23 to +38 cm. The CICE-free simulations also
527 show anomalously thinner and thicker ice during these years, but larger anomalies were
528 simulated in 2012 and 2014.

529 While the overall pattern of years with anomalously thin or thick ice is broadly similar
530 between the three CS2 products, this is not true in 2016. Both the CPOM and AWI thickness
531 estimates suggest slightly thicker ice than average (+4 cm and +9 cm, respectively), while the
532 NASA product suggests the icepack was overall slightly thinner (-1 cm). The CICE-free run is in
533 agreement with the NASA data set for the 2016 anomaly. Turning back to Figure 3, we find that
534 in 2016 the CPOM data set shows +20 to +60 cm thicker ice north of the Canadian Archipelago
535 (CAA) and Greenland, -20 to -60 cm thinner ice on the Pacific side of the pole, and +10 to +30
536 cm thicker ice north of the Laptev Sea. These spatial patterns of November 2016 SIT anomalies
537 are broadly similar with those from AWI but less so with NASA. However, despite similar
538 patterns of positive and negative thickness anomalies, AWI shows between +20 and +30 cm
539 thicker ice over much of the central Arctic Ocean, and even thicker ice (up to +60 cm) north of
540 the CAA and Greenland in November 2016 than the CPOM product. NASA on the other hand
541 shows larger negative anomalies on the Pacific side of the north pole of up to -70 cm and larger
542 positive anomalies directly north of the CAA between +10 and +20 cm.

543 Since we use CPOM CS2 thickness fields to initialize our CICE model runs, this comparison
544 is useful in determining whether or not the 2016 November thickness anomalies are robust in
545 other CS2 processing streams and provides a measure of CS2 sea ice thickness uncertainty.
546 However, since we do not have the AWI and NASA ITDs we cannot quantify the impact of
547 using a different thickness data set on our simulations. However, as a result of the negative

Formatted: Right: 0.25"



548
549
550
551
552

Figure 3. November ice thickness anomaly relative to 2010-2016 in cm based on CryoSat-2 data from UCL CPOM (left), Alfred Wegener Institute (AWI) (middle) and NASA (right). Grid points with less than 100 individual measurements and a mean sea ice thickness of less than 0.5 m are not included. CICE-free thickness anomalies are also shown in the left right column.

Formatted: Right: 0.25"

553 winter ice growth feedback (discussed below), differences due to model initialization in
554 November will be attenuated until April.

556 *Sea Ice growth from November to April*

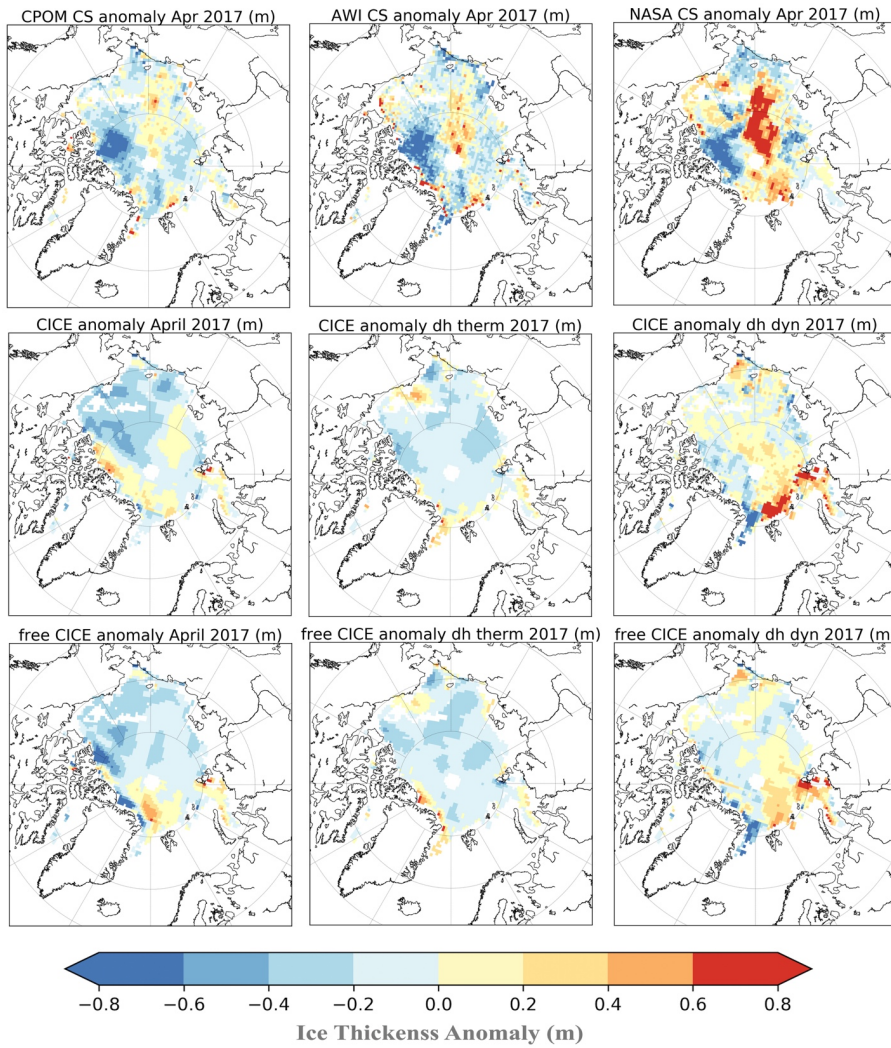
557 For a more robust analysis of winter ice growth during the record warm winter of 2016/2017,
558 we now include April thickness estimates from CS2 (CPOM, AWI and NASA), the free CICE
559 simulation and the CICE simulations initialized with CPOM CS2 November SIT in **Figure 4**.
560 Corresponding values for all other years are shown in **Figure 5** (CS2) and **Figure 6** (CICE).
561 **Table 3** summarizes associated mean April thickness and anomalies since 2011, together with
562 contributions from thermodynamics (ice growth) and dynamics (ice transport and ridging) based
563 on the CICE model simulations. The area for which these estimates are provided corresponds to
564 the area shown in Figure 1(d).

565 We first note that all 5 estimates have different strengths and weaknesses: while the mean
566 annual cycle of sea ice thickness *should* be more accurate from CS2 than modeled estimates,
567 robust analysis of winter ice growth from CS2 is in part limited due to the impact of
568 climatological snow depth assumptions, which may differ from one year to the next, and
569 differences in waveform processing between CS2 data providers, which may result in
570 inconsistencies in the magnitude and direction of the observed thickness anomalies. In the free
571 CICE simulation, November sea ice thickness is less certain due to error accumulation during the
572 model run. In the initialized CICE simulation, both these error sources are reduced but inherent
573 model biases remain. While we discuss some of the regional differences below, we are most
574 confident in the model simulations on the Arctic Basin-wide scale over which CICE has been
575 tuned to agree with CS2 winter ice growth.

576 Despite these limitations, all five approaches show good agreement in most years regarding
577 the direction of the thickness anomalies (i.e. positive or negative) even if they disagree on
578 absolute magnitude. For example, Arctic Ocean mean thickness anomalies are negative in all 3
579 CS2 products for April 2013 (ranging from -3 to -25 cm), whereas in April 2014 and 2015 all
580 approaches give positive mean thickness anomalies, ranging from +5 to +20 cm in 2014 and +11
581 to +22 cm in 2015 [**Table 3**]. In some years, the CICE-free simulation better matches the
582 observed April thickness anomalies (e.g. 2013, 2015), whereas in other years CICE-ini performs
583 better (e.g. 2012, 2014). On the other hand, in 2011 and 2017 we find disagreement among the
584 three CS2 data sets. In April 2011, both the CPOM and NASA product have overall negative
585 thickness anomalies for the Arctic Basin (-4 and -8 cm, respectively), whereas they are positive
586 in the AWI product (+7 cm). In April 2017, both the CPOM and AWI are in close agreement that
587 the ice cover was overall thinner (-13 and -12 cm, respectively), as are the CICE-free and CICE-
588 ini simulations (negative thickness anomalies of -13 cm), whereas NASA shows a weak positive
589 anomaly (+3cm).

590 Focusing more on April 2017, the 3 CS2 products suggest widespread thinner ice in April
591 2017 north of Ellesmere Island (up to -80 cm thinner) relative to the 2011-2017 mean [Figure
592 4(top)]. Thinner ice is also found within the Chukchi and East Siberian seas (on average -10 to -
593 35 cm thinner) despite a mix of positive and negative anomalies, CICE simulations on the other
594 hand show more widespread thinning throughout the western Arctic, including the Beaufort Sea
595 and positive thickness anomalies north of Ellesmere Island [Figure 4(middle and bottom)]. In
596 the Beaufort Sea, there is general disagreement among the 3 CS2 products as well as with the
597 CS2 results and the CICE simulations: regional mean anomaly of -5 cm (CPOM), 0 cm (AWI),
598 +20 cm (NASA), -25 cm (CICE-ini) and -30 cm (CICE-free). North of Ellesmere Island, CICE-

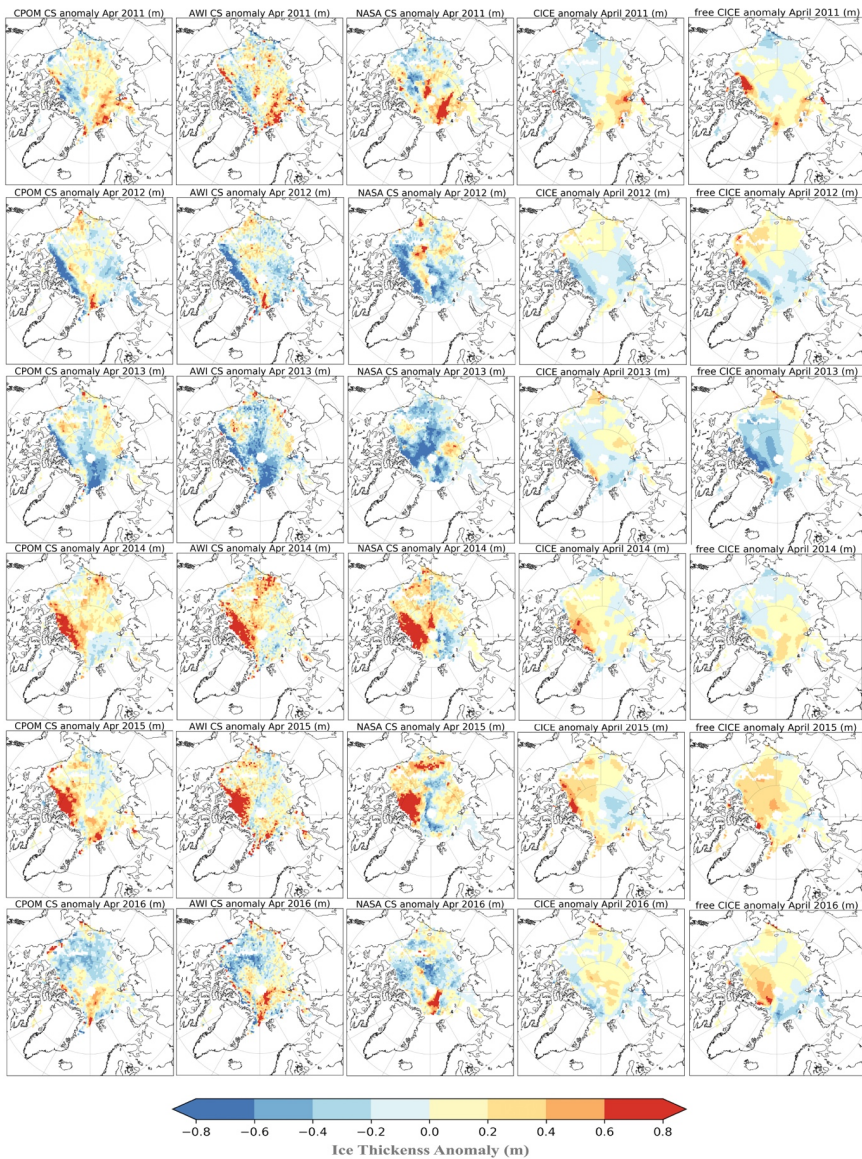
Formatted: Font:Bold
Deleted: sea ice within
Deleted: was
Deleted: in April 2017 compared to the 2011-2017 mean
Deleted: [Figure 4(top)]
Deleted: There is also disagreement n
Deleted: of the CAA
Deleted: with
Formatted: Right: 0.25"



606
607
608
609
610
611
612

Figure 4. CryoSat-2 and CICE simulated thickness anomalies in April 2017 relative to the 2011-2017 mean. Top images show the total ice thickness anomalies from CryoSat-2 for CPOM (left), AWI (middle) and NASA (right). The middle left image shows April 2017 thickness anomalies from CICE initialized with CPOM November CS2 thickness together with the contributions from thermodynamics (middle) and dynamics (left) and bottom show the corresponding results from the CICE free simulations. Grid points with less than 100 individual measurements and a mean sea ice thickness of less than 0.5 m are not included.

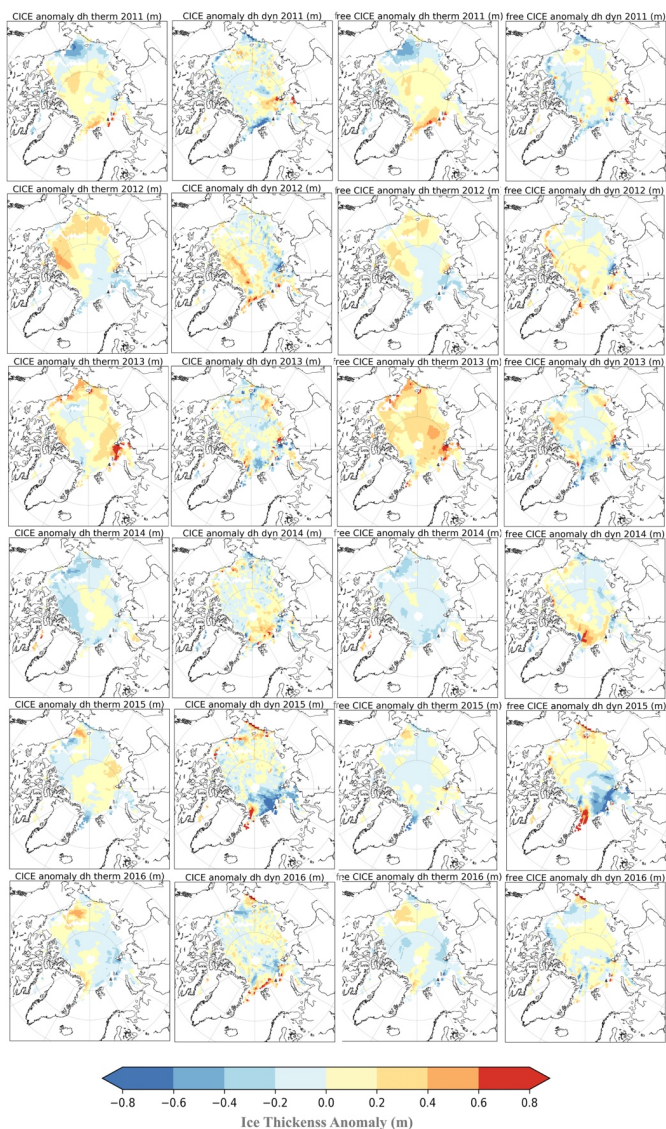
Formatted: Right: 0.25"



613
614
615
616
617

Figure 5. Anomaly of April ice thickness from 2011 to 2016 in m relative to the 2011 to 2017 mean from CryoSat-2 CPOM (far left), AWI (second left), NASA (middle), CICE simulations initialized with November CPOM CryoSat-2 thickness fields (2nd right), and CICE simulations not initialized with CryoSat-2 thickness (right). Grid points with less than 100 individual measurements and a mean sea ice thickness of less than 0.5 m are not included.

Formatted: Right: 0.25"



619
620
621
622
623

Figure 6. Anomalies of CICE simulated thermodynamic ice growth and dynamical thickness changes in m relative to the 2011 to 2017 mean from the CICE simulations initialized with November CPOM CryoSat-2 thickness fields (left), and CICE simulations not initialized with CryoSat-2 thickness (right). The year in title reflects the end month over which ice growth occurs (e.g. from November to April).

Formatted: Right: 0.25"

624
625
626
627
628
629
630
631
632
633
634
635
636
637
638
639
640
641
642
643
644
645
646
647
648
649

ini indicates positive thickness anomalies (up to +50 cm), whereas all 3 CS2 products show negative thickness anomalies (up to -80 cm). In this region, the CICE-free simulation also shows mostly negative thickness anomalies (-20 to -80 cm), with a small positive area (up to +25 cm).

While the discrepancy in this region is puzzling, the bias between the CICE-*ini* simulations and the CS2 products may in part reflect the use of a snow climatology in the CS2 thickness retrievals. As discussed earlier, a positive sea ice thickness anomaly was found in the November 2016 CS2 thickness retrievals north of CAA and Greenland. Yet this positive thickness anomaly is not preserved through April in both the CPOM and AWI CS2 products. **Figure 7** shows CICE simulated snow depth anomalies in November 2016 and April 2017. In November, small positive snow depth anomalies occur throughout the Arctic, especially north of the Queen Elizabeth Islands where the anomaly locally increases to 20 cm. By April, the anomalies cover a broader region and increase in magnitude. A positive April snow depth anomaly of 15 to 20 cm relative to *W99* would result in an underestimation of the CS2-retrieved April ice thickness (SIT) by 88 to 115 cm using the following equation:

$$SIT = \frac{\rho_{snow}H_{snow} + \rho_{water}F_c}{(\rho_{water} - \rho_{ice})}$$

where F_c is the corrected radar freeboard (F_b) for the reduced propagation of the speed of light through the snow cover ($F_c = F_b + 0.25H_{snow}$) [Tilling *et al.*, 2017], and using a snow density (ρ_{snow}) of 320 kg/m³ [Warren *et al.*, 1999], ice density (ρ_{ice}) of 915 kg/m³, water density of (ρ_{water}) 1024 kg/m³. CICE-*ini*, which relies on the CPOM CS2 November thickness, maintains this positive thickness anomaly through April despite thermodynamic ice growth. The CICE-free simulation on the other hand started with negative thickness anomalies in November within this region, and maintains them through April.

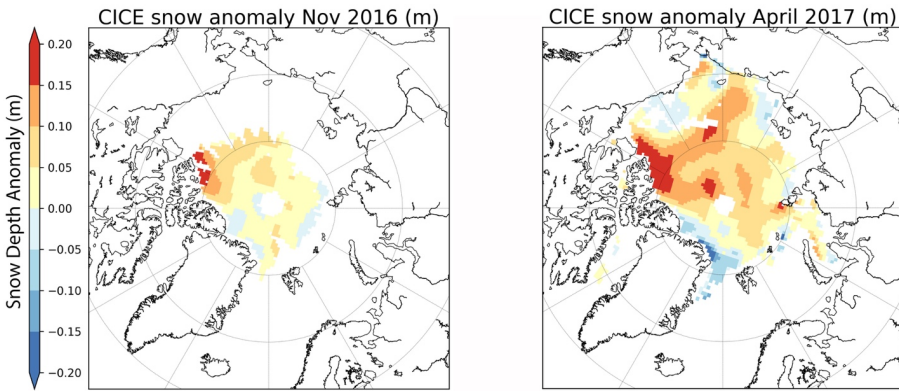


Figure 7. Snow depth anomaly for November 2016 (relative to 2010-2016) and April 2017 (relative to 2011-2017) from CICE.

650
651
652
653

Deleted: ing
Deleted: generally

Deleted: may

Formatted: Font: 10 pt

Formatted: Right: 0.25"

657 On the other hand, thickness is also strongly influenced by dynamics, such as convergence
658 against the CAA and Greenland which leads to thicker ice in this region [Kwok et al., 2015].
659 During winter 2017 however, the Beaufort High largely collapsed, reducing convergence against
660 the northern CAA and Greenland [Figure 8]. One advantage of using CICE, is that we can more
661 readily diagnose thermodynamic vs. dynamical contributions to the observed thickness
662 anomalies. For the region directly north of Ellesmere Island, both the CICE-ini and CICE-free
663 simulations support reduced sea ice convergence, leading to thinner ice from dynamical
664 contributions. At the same time, this region also exhibited reduced thermodynamic ice growth in
665 both CICE simulations. One would expect thermodynamic ice growth to be reduced in regions of
666 enhanced snow depth and thicker November ice. Positive snow depth anomalies extended from
667 this region through the northern Beaufort Sea, in agreement with extended regions reductions in
668 thermodynamic ice growth in both CICE-free and CICE-ini. At the same time, regions of
669 positive 2016 November thickness anomalies are also associated with regions of reduced CICE
670 thermodynamic ice growth.

671 Overall, the largest reductions in thermodynamic ice growth during winter 2016/2017
672 occurred within the Chukchi Sea and north of the CAA, extending through the northern Beaufort
673 Sea (on the order of -40 cm). While snow depth and thickness anomalies influenced
674 thermodynamic ice growth north of the CCA, within the Chukchi Sea the negative ice growth
675 anomalies was a result of late ice formation: ice formed a month later than the 1981-2010 mean
676 within the Chukchi Sea. This seems to have been more important than increases in ice thickness
677 from dynamics. Dynamical thickness changes simulated by CICE show an overall thickening of
678 the ice in winter 2016/2017 within the Chukchi and Bering seas (up to 50 cm). Anomalous
679 ridging in this region is in agreement with observed high amounts of deformation along the shore
680 fast ice zone within the Chukchi Sea as a result of persistent west winds from December to
681 March (<http://arcus.org/sipn/sea-ice-outlook/2017/june>).

682 An exception to reduced thermodynamic ice growth occurs directly north of Utqiagvik,
683 Alaska (formerly Barrow), with positive thermodynamic ice growth anomalies of 30 to 40 cm.
684 This enhanced ice growth was offset by ice divergence, leading to overall thinner ice in the CICE
685 simulations. In situ observations of level first-year ice thickness off the coast of Utqiagvik
686 ranged between 1.35 and 1.40m during May (<http://arcus.org/sipn/sea-ice-outlook/2017/june>)
687 and appear to be in better agreement with the CICE simulations, as well as the CPOM and AWI
688 CS2 thickness estimates, while the NASA CS2 product shows positive thickness anomalies in
689 that region. Positive thermodynamic ice growth anomalies are also found for small regions north
690 of Greenland and within Fram Strait, as well as within some scattered coastal regions of the
691 Chukchi, East Siberian, Laptev and Kara seas.

692 Finally, large dynamical thickening was found within the Kara and northern Barents seas (up
693 to 1.2 m) and to a lesser extent over the southern and western Greenland Sea, Baffin Bay and the
694 Labrador Sea (not shown). The CICE-simulated dynamical thickening in the Barents and Kara
695 seas is more anomalous than seen during previous CS2 years [Figure 6], and likely reflects the
696 influence of the positive Arctic Oscillation (AO) on ice motion [Figure 8]. The AO was positive
697 from December through March, a pattern which results in offshore ice advection from Siberia
698 and enhanced ice advection through Fram Strait [Rigor et al., 2002]. This pattern leads to
699 development of thin ice in newly formed open water areas, increasing thermodynamic ice growth
700 in the Laptev Sea, whereas increased ice advection from thick ice regions north of Greenland
701 towards Fram Strait, combined with changes in internal ice stress as the ice cover has thinned,
702 leads to more deformation. Interestingly, while the CICE model runs confirm overall slightly

Formatted: Font:Italic

Deleted: - ... [1]

Formatted: Font:Bold

Moved (insertion) [1]

Deleted: Spatially,

Deleted: and

Deleted: These regions have very different explanations for reduced thermodynamic ice growth.

Deleted: I

Deleted: , reducing the number of days over which the ice could grow. In contrast, north of the CAA, winter ice growth was reduced in a region that showed positive November thickness anomalies, illustrating the strong dependence of thermodynamic ice growth on initial ice thickness. This region also had anomalously positive snow depths that extended through the northern Beaufort Sea, in agreement with extended regions of reduced thermodynamic ice growth

Formatted: Font:Italic

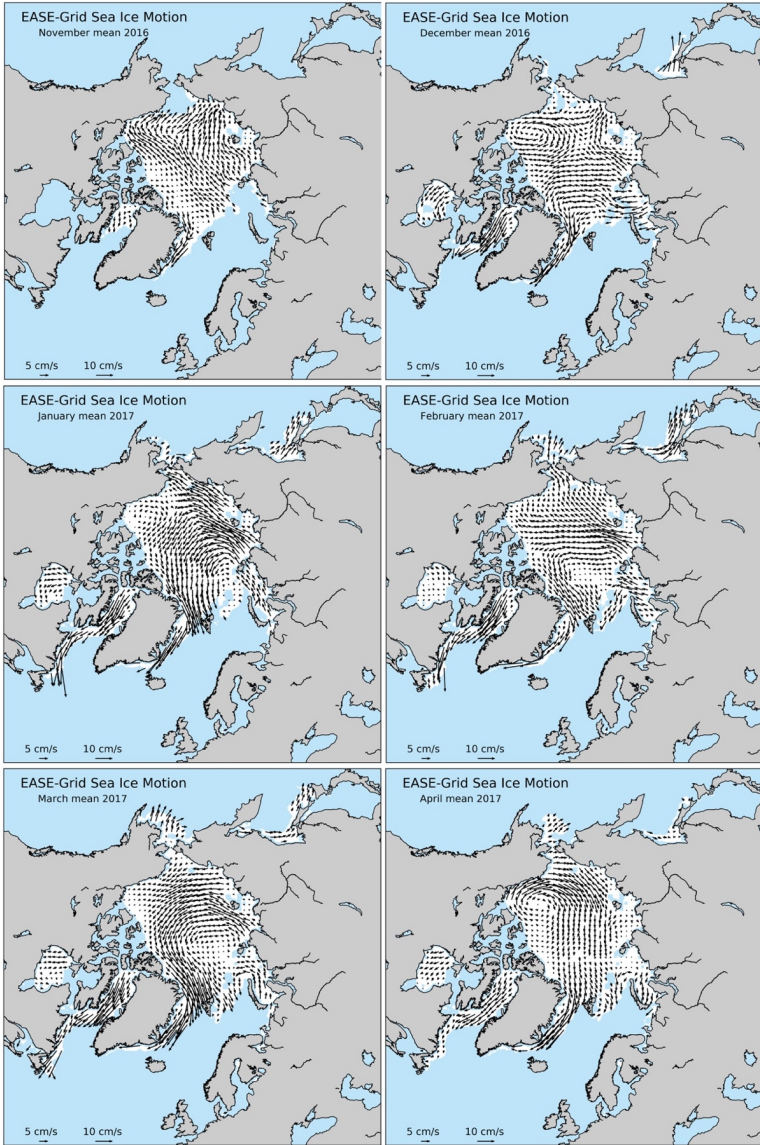
Deleted: - ... [2]

Moved up [1]: One would expect thermodynamic ice growth to be reduced in regions of enhanced snow depth and thicker November ice. Spatially, the largest reductions in thermodynamic ice growth during winter 2016/2017 occurred within the Chukchi Sea and north of the CAA and extending through the northern Beaufort Sea (on the order of -40 cm). These regions have very different explanations for reduced thermodynamic ice growth. Ice formed a month later than the 1981-2010 mean within the Chukchi Sea, reducing the number of days over which the ice could grow. In contrast, north of the CAA, winter ice growth was reduced in a region that showed positive November thickness anomalies, illustrating the strong dependence of thermodynamic ice growth on initial ice thickness. This region also had anomalously positive snow depths that extended through the northern Beaufort Sea, in agreement with extended regions of reduced thermodynamic ice growth.

Deleted: dynamical thickness changes simulated by CICE show an overall thickening of the ice in winter 2016/2017 particularly within the Chukchi and Bering seas (up to 50 cm). Anomalous ridging in this region is in agreement with observed high amounts of deformation along the shore fast ice zone within the Chukchi Sea as a result of persistent west winds from December to March (<http://arcus.org/sipn/sea-ice-outlook/2017/june>). Even

Deleted: r

Formatted: Right: 0.25"



748
749
750

Figure 8. Mean monthly sea ice motion from the NSIDC Polar Pathfinder Data Set. Preliminary data provided by Scott Stewart, NSIDC.

Formatted: Right: 0.25"

751 thinner ice within the Barents Sea in April 2016, consistent with the studies by *Ricker et al.*
752 [2017a] and *Boisvert et al.* [2016], the thinning from reduced thermodynamic ice growth was
753 largely offset by thickening from dynamical effects [Figures 5 and 6].
754

755 Overall, for the Arctic Basin as a whole, CICE simulations suggest the overall thinner ice
756 observed in April 2017 is largely result of reduced thermodynamic ice growth (-11 to -13 cm),
757 with dynamics adding +1 to +4 cm [Table 3].

758
759 **Negative feedbacks**

760 Ice growth after the September minima is a result of turbulent heat flux exchanges between
761 the relatively warm ocean mixed layer and the cold autumn and winter air through the snow-
762 covered sea ice. Progressively, as the ice grows to about 1.5 to 2 m thick, the ocean becomes
763 well insulated from the atmosphere and ice growth is slowed. Thus, it is not surprising that we
764 see less thermodynamic ice growth in regions of relatively thick (> 2.5 m) November ice. A case
765 in point is seen in winter 2013/2014 when thermodynamic ice growth was reduced by 9 to 10
766 cm, despite an overall colder winter.

767 On the other hand, thinner ice regions generally exhibit more vigorous ice growth. For
768 example, during winter 2012/2013, CICE-free, and to a lesser extent CICE-ini simulated
769 thermodynamic ice growth increased throughout much of the Arctic Ocean in areas where the ice
770 retreated in September 2012 [Figure 6] and where the November 2012 thickness anomalies were
771 negative [Figure 3]. This process of rapid winter ice growth over thin ice regions represents a
772 negative feedback, allowing for ice to form quickly over large parts of the Arctic Ocean
773 following summers with reduced ice cover and thinner November ice.

774 Thus, while summer sea ice is rapidly declining, several studies have indicated negative
775 feedbacks over winter continue to dominate [e.g. *Notz and Marotzke*, 2012; *Stroeve and Notz*,
776 2015], allowing for recovery following summers with anomalously low sea ice extent, such as
777 those observed in 2007 and 2012. This is further supported in the CICE-free simulations which
778 show the least amount of winter ice growth for the Arctic Basin in 1989, and peak ice growth
779 following the 2007 and 2012 record minimum sea ice extent [Figure 9]. As a result, mean ice
780 growth from November to April in CICE simulations from 1985 to 2017 shows a positive trend
781 that is weakly correlated to winter air temperatures or FDDs ($R=0.49$). On the other hand, we
782 find a strong inverse correlation ($R=-0.82$) between November sea ice thickness and winter ice
783 growth. Thus, because thin ice grows faster than thick ice, there is an overall stabilizing effect
784 that suggests as long as air temperatures remain below freezing, even if they are anomalously
785 warm, the ice can recover during winter. This stabilizing feedback over winter means that major
786 departures of the September sea ice extent from the long-term trend caused by summer
787 atmospheric variability generally does not persist for more than a few years [*Serreze and*
788 *Stroeve*, 2015].

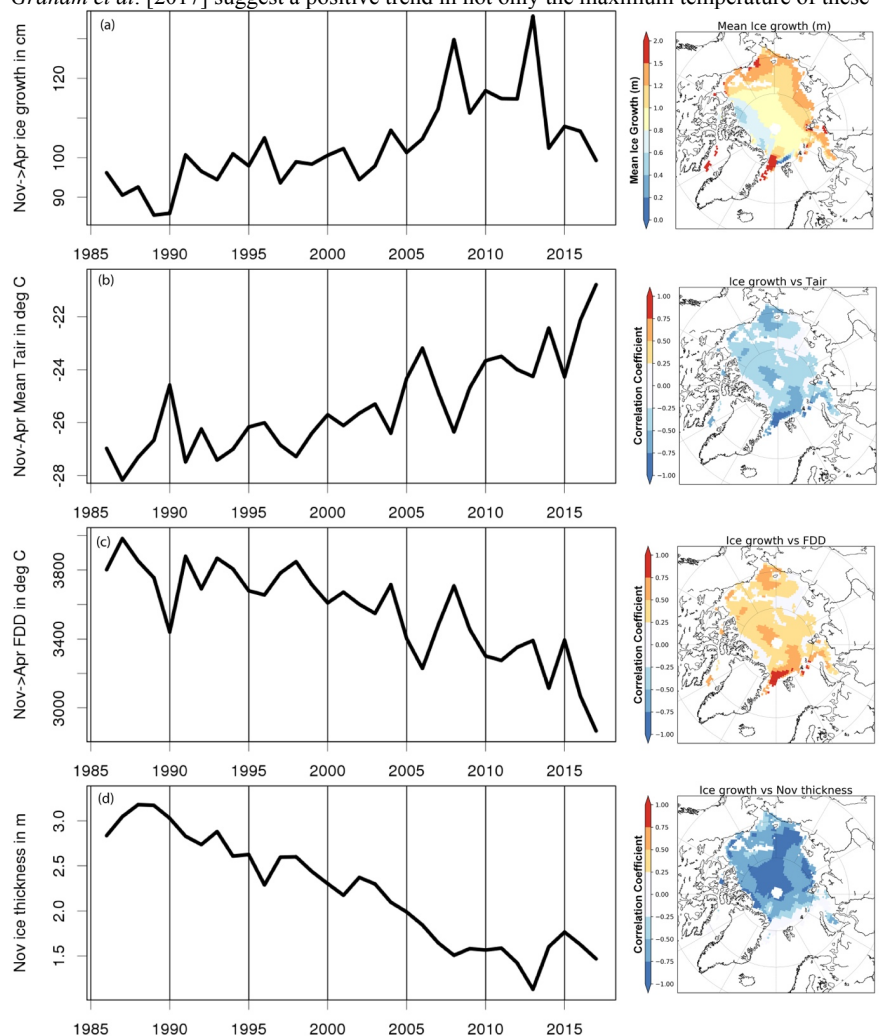
789 However, since 2012, overall ice growth has declined as winter air temperatures have
790 increased further. This not surprising in that there was a lot of new ice to form in the open waters
791 left after the 2012 record minima. However, 2016 tied with 2007 for the second lowest Arctic sea
792 ice minimum and overall thermodynamic ice growth was significantly less. The correlation from
793 1985 to 2012 is smaller than over the full record ($R=0.34$), suggesting a growing influence of
794 warmer winter air temperatures though the difference in correlation is not statistically significant.
795 While there remains a large amount of inter-annual variability in winter warming events,

Formatted: Font:Bold

Deleted: -

Formatted: Right: 0.25"

797 Graham et al. [2017] suggest a positive trend in not only the maximum temperature of these



798
799 **Figure 9.** Time-series from 1985 to 2017 of mean winter ice growth (mid-November to mid-April) in the free CICE
800 simulation (a), mean 2m NCEP-2 air temperature (b), cumulative freezing degree days (FDDs) (c) and November ice
801 thickness (d). All time-series results are averaged over the areas shown in Figure S1(c). Corresponding images to
802 the left of each time-series plots show: mean ice growth from November to April as averaged from 1985/1986 to
803 2016/2017; correlation coefficient between ice growth and 2m NCEP-2 air temperature; correlation coefficient
804 between ice growth and FDDs; and correlation coefficient between ice growth and November ice thickness,
805 respectively. All correlation values are given for linear regression of de-trended time series.

Formatted: Right: 0.25"

806 warming events, but also in their duration. Interestingly, there is a modest correlation between
807 detrended FDDs and the winter maxima sea ice extent ($R=0.30$); not removing the trend results
808 in a correlation of $R=0.83$. Thus, recent reductions in overall FDDs may have played a role in the
809 last three years of record low maxima extents.

810

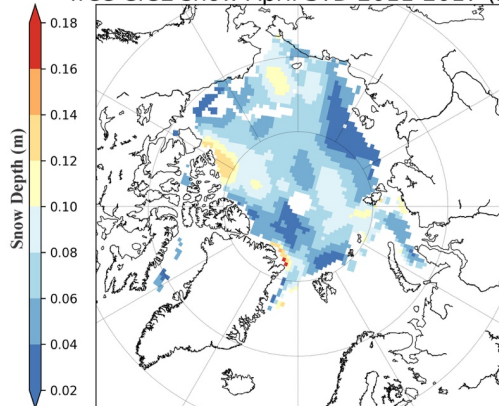
811

Discussion

812

813 The CICE-simulations and CS2 thickness retrievals from CPOM and AWI show consistency
814 that the Arctic Basin sea ice cover in April 2017 was on average 13 cm thinner than the 2011-
815 2017 mean. However, it ~~may not have been~~ the thinnest during the CS2 data record. Thickness
816 retrievals from the different CS2 data sets showed larger negative thickness anomalies in April
817 2013, ranging from -13 to -25 cm, whereas the CICE simulations showed smaller anomalies (-3
818 to -12 cm). While we expect retrievals from satellite to be more accurate than those from model
819 simulations, whether or not a year is anomalously low relative to another year will depend in part
820 on the inter-annual variability in the snow cover. All three CS2 products rely on the W99 snow
821 depth climatology. While Haas et al. (2017) found snow depth within the Lincoln Sea in 2017
822 was similar to W99, evaluation of reanalysis data shows considerable variability in total
823 precipitation from year to year [Barrett et al., submitted]. In the CICE-free simulations, snow
824 depth is modeled using precipitation from NCEP-2. Inter-annual variability from April 2011 to
825 April 2017 (calculated as standard deviation between the 7 monthly April means) is shown in
826 **Figure 10**. North of the CAA, standard deviations in snow depth are on the order of 12 to 14 cm,
827 whereas other regions are on the order of 2 to 12 cm. From the W99 climatology, inter-annual
828 variability in snow depth during the winter months was estimated to be only 4 to 6 cm,
829 significantly less than what is exhibited here. Since ice thickness increases approximately 6 times
830 the snow depth uncertainty, a 12 to 14 cm uncertainty would lead to 72 to 83 cm increase in
831 CS2-derived ice thickness. If we average for the area shown in Figure 1(d), snow depth
832 anomalies ranged from -6 cm to +6 cm, with a corresponding impact of -41 to +41 cm on
833 thickness.

free CICE snow April STD 2011-2017 (m)



833

834

835

836

Figure 10. Standard deviation of CICE-simulated snow depth using NCEP-2 reanalysis for the month of April from 2011 to 2017.

Deleted: was likely

Deleted: not

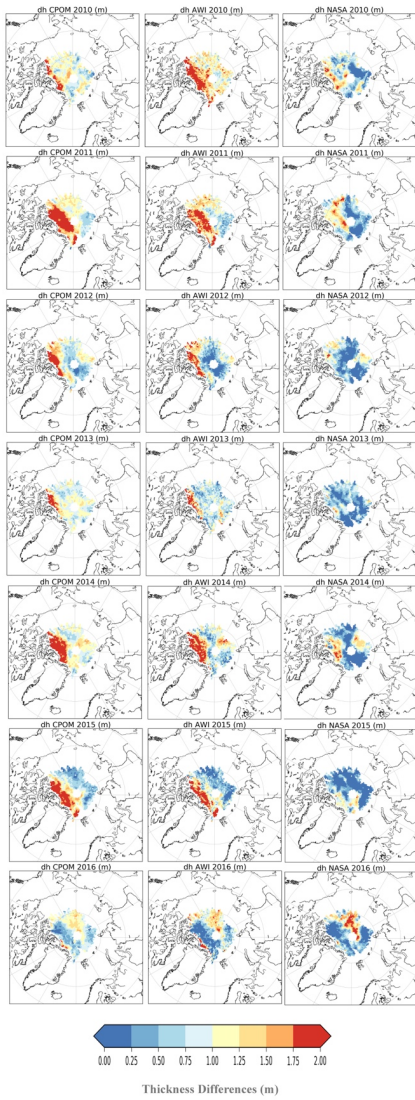
Deleted: thickness anomalies were mostly larger than in 2016

Deleted: much

Formatted: Font: Italic

Deleted: However, precipitation varies considerably from one year to the next.

Formatted: Right: 0.25"



844
 845 **Figure 11.** Comparison between ice growth (April minus November) in the UCL CPOM CryoSat-2 thickness
 846 retrievals (left) and those from the Alfred Wegener Institute (AWI) (middle) and NASA (right). The year shown
 847 corresponds to the November months, such that 2016 refers to ice thickness differences between April 2017 and
 848 November 2016. Results are only shown for the area shown in Figure 1(c), which represents grid points that had
 849 more than 100 individual measurements and a mean sea ice thickness greater than 0.5 m during the November
 850 months.

Formatted: Right: 0.25"

§51

852 Besides not accounting for inter-annual variability in snow depth, which makes assessing
853 thickness anomalies from one year to the next less certain, differences in waveform processing
854 between the three different CS2 products adds further uncertainty. The fact that the NASA CS2
855 product is a general outlier compared to the AWI and CPOM products is further highlighted in
856 **Figure 11**. Across the area considered (e.g. areas in color shown in Figure 1(c)), the difference
857 between April and the previous November ice thickness is shown for each CryoSat-2 year. The
858 AWI and CPOM products tend to exhibit positive ice growth over winter, focused north of
859 Greenland and the CAA and sometimes also across the pole. The NASA product on the other
860 hand generally shows less ice growth between November and April in most years, and even no
861 ice growth in some regions. The reasons for this are unclear, yet interestingly in winter
862 2016/2017, all three products show more agreement in regards to thickness decreases that span a
863 broad region north of Greenland and the CAA, combined with positive increases south of the
864 pole towards the East Siberian and Laptev seas.

865 Finally, how important were the April thickness anomalies in the evolution of the summer ice
866 cover in summer 2017? Several studies have discussed how thin winter ice may precondition the
867 Arctic for less sea ice at the end of the melt season as thinner ice melts and open water areas
868 form more readily in summer, enhancing the ice albedo feedback [e.g. *Stroeve et al.*, 2012;
869 *Perovich et al.*, 2008], and sea ice thickness has been used as a predictor for the September sea
870 ice extent [*Kimura et al.*, 2013]. Thus, we may have expected 2017 to be among the lowest
871 recorded sea ice extents as the ice cover was likely thinner than average and the winter extent
872 was the lowest in the satellite record. Nevertheless, the minimum extent ended up as the 8th
873 lowest in the satellite data record. This highlights the continuing importance of summer weather
874 patterns in driving the September minimum. Spring and summer 2017 were dominated by
875 several cold core cyclones, leading to near average air temperatures and ice divergence [see
876 <http://nsidc.org/arcticseaicenews/> for a discussion of this summer's weather patterns]. Overall,
877 the correlation between detrended winter sea ice thickness anomalies and September sea ice
878 extent remains low [*Stroeve and Notz*, 2015]. Other factors such as melt pond formation in
879 spring [*Schröder et al.*, 2014] and summer weather patterns still largely govern the evolution of
880 the summer ice pack at current thickness levels [e.g. *Holland and Stroeve*, 2011]. Interestingly,
881 predictions of the monthly mean September 2017 sea ice extent based on spring melt pond
882 fraction in May gave a value of 5.0 ± 0.5 million km², whereas the observed value was 4.80
883 million km² [See arcus.org/sign/sea-ice-outlook/2017/june].
884

885 Conclusions

886 In this study we examined sea ice thickness anomalies derived from three different CS2 data
887 products and that simulated using CICE. Overall freezing degree days were much reduced in
888 winter 2016/2017, and subsequent sea ice thickness estimates from CryoSat-2 in April 2017
889 suggest the ice was thinner over large parts of the Arctic Ocean. These results are complimented
890 with CICE model simulations, both with and without initializing with November ice thickness
891 distributions from CS2. While CICE simulations suggest the mean thickness within the Arctic
892 Basin in April 2017 was the thinnest over the CryoSat-2 data record, corresponding CS2-derived
893 sea ice thickness from the three different data providers put this into question. However, the use
894 of CS2-derived freeboards with a snow depth climatology remains problematic because it fails to
895 capture inter-annual snow accumulation variability. Differences in processing of the radar
896 waveform, values of snow and ice density, delineation of first-year vs. multiyear ice, and sea

Deleted: which remains a large source of error in current CS2 thickness retrievals

Formatted: Right: 0.25"

899 surface height retrieval also contribute to differences among available data sets, making it
900 challenging to robustly assess inter-annual variability of ice thickness from CryoSat-2. Despite
901 these challenges it is encouraging that in most years, the interannual variability in positive and
902 negative anomalies is consistent between the 3 CS2 data sets.

903 Finally, CICE-free simulations from 1985 to 2017 reveal the correlation between winter ice
904 growth and November ice thickness ($R=-0.82$) is stronger than between growth and FDDs
905 ($R=0.49$), highlighting the importance of the negative winter growth feedback mechanism. This
906 supports previous studies that the long-term sea ice reduction in the Arctic Basin is mainly
907 driven by summer atmospheric conditions. However, this correlation has become weaker since
908 2012, indicating that higher winter air temperatures and further delays in autumn/winter freeze-
909 up due to warmer mixed-layer ocean temperatures prohibit a complete recovery of winter ice
910 thickness in spite of the negative feedback mechanism. This is highlighted by the fact that overall
911 thermodynamic ice growth for winter 2016/2017 was just under 1m despite 2016 reaching the
912 second lowest minimum extent recorded during the satellite record.

914 Acknowledgements

915 This work was in part funded under NASA grant NNX16AJ92G (Stroeve). Sea ice simulations
916 and CryoSat-2 satellite data processing performed under NERC funding of the Centre for Polar
917 Observation and Modeling (CPOM). CryoSat-2 thickness fields courtesy of A. Ridout at CPOM.
918 Processing of the AWI CryoSat-2 (PARAMETER) is funded by the German Ministry of
919 Economics Affairs and Energy (grant: 50EE1008) and data from November 2010 to April 2017
920 obtained from <http://www.meereisportal.de> (grant: REKLIM-2013-04). NASA CryoSat-2 data
921 provided courtesy of Nathan Kurtz. NCEP2 data obtained from NOAA Earth System Research
922 Laboratory (<http://www.esrl.noaa.gov/psd/data/gridded/data.ncep.reanalysis2.gaussian.html>).
923 Data policy: data available upon request.

925 References

- 926 Bekryaev, R.V., I.V. Polyakov and V.A. Alexeev (2010), Role of polar amplification in long-
927 term surface air temperature variations and modern Arctic warming, *J. Clim.*, 23, 3888-3906.
928 Bitz, C.M. and G.H. Roe (2004), A mechanism for the high rate of sea ice thinning in the Arctic
929 Ocean, *J. Clim.*, 17, 2623-2632, doi:10.1175/1520-0442(2004)017<3623:AMFTHR>2.0.CO;2.
930 Boisvert, L.N., A.A. Petty, and J. Stroeve (2016), The Impact of the Extreme Winter 2015/16
931 Arctic Cyclone on the Barents–Kara Seas, *Bull. Amer. Met. Soc.*, doi:10.1175/MWR-D-16-
932 0234.1.
933 Cohen, L., S. R. Hudson, V. P. Walden, R. M. Graham, M. A. Granskog (2017), Meteorological
934 conditions in a thinner Arctic sea ice regime from winter through early summer during the
935 388 Norwegian young sea ICE expedition (N-ICE2015), *J. Geophys. Res. Atmos.*,
936 doi:10.1002/2016JD026034.
937 Cullather, R. I., Y. Lim, L. N. Boisvert, L. Brucker, J. N. Lee, and S. M. J. Nowicki (2016),
938 Analysis of the 426 warmest Arctic winter, 2015-2016, *Geophys. Res. Lett.*, 808–816,
939 doi:10.1002/2016GL071228.
940 Dee, D. P. et al. (2011), The ERA-Interim reanalysis: Configuration and performance of the data
941 428 assimilation system, *Q. J. R. Meteorol. Soc.*, 137(656), 553–597, doi:10.1002/qj.828.
942 Flocco, D., D. Schröder, D. L. Feltham, and E. C. Hunke (2012), Impact of melt ponds on Arctic
943 sea ice simulations from 1990 to 2007, *J. Geophys. Res.*, doi:10.1029/2012JC008195.

Deleted:

Formatted: Default Paragraph Font, Font:Font color: Auto, Pattern: Clear

Formatted: Right: 0.25"

945 Graham, R.M., L. Cohen, A.A. Petty, L.N. Boisvert, A. Rinke, S.R. Hudson, M. Nicolaus and
 946 M.A. Granskog, (2017), increasing frequency and duration of Arctic winter warming events,
 947 *Geophys. Res. Lett.*, **16**, 6974-6983, doi:10.1002/2017GL073395.

948 Graversen, R.G. and M. Burtu (2016), Arctic amplification enhanced by latent energy transport
 949 of atmospheric planetary waves, *Quart. Royal Meteor. Soc.*, doi:10.1002/qj.2802.

950 Graversen RG. 2006. Do changes in midlatitude circulation have any impact on the Arctic
 951 surface air temperature trend? *J. Clim.* **19**: 5422–5438.

952 Haas, C., Beckers, J., King, J., Silis, A., Stroeve, J., Wilkinson, J., Notenboom, B., Schweiger,
 953 A., & Hendricks, S. (2017). Ice and snow thickness variability and change in the high Arctic
 954 Ocean observed by in situ measurements. *Geophys. Res. Lett.*, **44**, 10,462–10,469,
 955 doi:10.1002/2017GL075434.

956 Hendricks, S., R. Ricker and V. Helm (2016), User Guide - AWI CryoSat-2 Sea Ice Thickness
 957 Data Product (v1.2).

958 Holland, M.M. and J.C. Stroeve (2011), Changing seasonal sea ice predictor relationships in a
 959 changing Arctic climate, *Geophys. Res. Lett.*, doi:10.1029/2011GL049303.

960 Hunke, E. C., W. H. Lipscomb, A. K. Turner, N. Jeffery, and S. Elliott (2015), CICE: the Los
 961 Alamos Sea Ice Model Documentation and Software User’s Manual Version 5.1.

962 Jakobshavn, E., T. Vihma, T. Palo, L. Jakobson, H. Keernik and J. Jaagus (2012), validation of
 963 atmospheric reanalysis over the central Arctic Ocean, *Geophys. Res. Lett.*, **39**, L10802,
 964 doi:10.1029/2012GL051591.

965 Kanamitsu, M., W. Ebisuzaki, J. Woollen, S-K Yang, J.J. Hnilo, M. Fiorino, and G. L. Potter
 966 (2002, updated 2017), NCEP-DOE AMIP-II Reanalysis (R-2): 1631-1643, *Bull. Amer. Met.*
 967 *Soc.*

968 Kimura, N., A. Nishimura, Y. Tanaka and H. Yamaguchi (2013), Influence of winter sea-ice
 969 motion on summer ice cover in the Arctic, *Polar Research*, **32**,
 970 doi:10.3402/polar.v32i0.20193.

971 Kurtz, N. and J. Harbeck. 2017. *CryoSat-2 Level 4 Sea Ice Elevation, Freeboard, and Thickness,*
 972 *Version 1.* [Indicate subset used]. Boulder, Colorado USA. NASA National Snow and Ice
 973 Data Center Distributed Active Archive Center. [Date Accessed].

974 Kurtz, N.T., N. Galin and M. Studinger (2014), An improved CryoSat-2 sea ice freeboard
 975 retrieval algorithm through the use of a waveform fitting, *The Cryosphere*, **8**, 1217-1237,
 976 doi:10.5194/tc-802017-2014.

977 Kwok, R. (2015). Sea ice convergence along the Arctic coasts of Greenland and the Canadian
 978 Arctic Archipelago: Variability and extremes (1992–2014), *Geophys. Res. Lett.*, **42**, 7598–
 979 7605, doi:10.1002/2015GL065462.

980 Laxon, S. W., K.A. Giles, A.L. Ridout, D.J. Wingham, R. Willatt, R. Cullen, R. Kwok, A.
 981 Schweiger, J. Zhang, C. Haas, S. Hendricks, R. Krishfield, N. Kurtz, S. Farrell, and M.
 982 Davidson, (2013), CryoSat-2 estimates of Arctic sea ice thickness and volume, *Geophys. Res.*
 983 *Lett.*, **40**, 732–737, doi:10.1002/grl.50193.

984 Markus, T., J. C. Stroeve, and J. Miller. (2009). Recent changes in Arctic sea ice melt onset,
 985 freeze-up, and melt season length, *J. Geophys. Res.*, doi:10.1029/2009JC005436.

986 Merkouriadi, I., B. Cheng, R.M. Graham, A. Rosel and M.A. Granskog (2017), Critical role of
 987 snow on sea ice growth in the Atlantic sector of the Arctic Ocean, *Geophysical Research*
 988 *Letters*, **44**, 10-479-10,485, doi:10.1002/2017GL075494.

989 Moore, G. W. K. (2016), The December 2015 North Pole Warming Event and the Increasing
 990 Occurrence of Such Events, *Sci. Rep.*, **6**(November), 39084, doi:10.1038/srep39084.

Formatted: Indent: Left: 0", Hanging: 0.2"

Formatted: Font color: Auto, Pattern: Clear

Formatted: Font color: Text 1

Formatted: Font:Font color: Text 1

Formatted: Font:Italic, Font color: Text 1

Formatted: Font:Font color: Text 1

Deleted: Laxon, S. W., K. A. Giles, A. L. Ridout, D. J. Wingham, R. Willatt, R. Cullen, R. Kwok, 393 A. Schweiger, J. Zhang, C. Haas, S. Hendricks, R. Krishfield, N. Kurtz, S. Farrell, 394 and M. Davidson (2013), Cryosat-2 estimates of arctic sea ice thickness and volume, 395 *Geophys. Res. Lett.*, **40** (4), 732–737, doi:10.1002/grl.50193.

Formatted: Font:(Default) Times New Roman, 12 pt

Formatted: Font:12 pt

Formatted: Right: 0.25"

997 Notz, D. and J. Marotzke (2012), Observations reveal external driver for Arctic sea ice retreat,
 998 *Geophys. Res. Lett.*, doi:10.1029/2012GL051094.
 999 Overland, J. E., and M. Wang (2016), Recent extreme arctic temperatures are due to a split polar
 1000 vortex, *J. Clim.*, 29(15), 5609–5616, doi:10.1175/JCLI-D-16-0320.1.
 1001 Perovich, D.K., J.A. Richter-Menge, K.F. Jones and B. Light (2008), Sunlight, water and ice:
 1002 Extreme Arctic sea ice melt during the summer of 2007, *Geophys. Res. Lett.*,
 1003 doi:10.1029/2008GL034007.
 1004 Pithan, F. and T. Mauritsen (2014), Arctic amplification dominated by temperature feedbacks in
 1005 contemporary climate models, *Nature Geoscience*, 7, 181-184, doi:10.1038/ngeo2017.
 1006 Polyakov I.V., A. Beszczynska, E.C. Carmack, I.A. Dmitrenko, E. Fahrbach, I.E. Frolov, R.
 1007 Gerdes, E. Hansen, J. Holfort, V.V. Ivanov, M.A. Johnson, M. Karcher, F. Kauker, J.
 1008 Morison, K.A. Orvik, U. Schauer, H.L. Simmons, A. Skagseth, V.T. Sokolov, M. Steele, L.A.
 1009 Timokhov, D. Walsh and J.E. Walsh (2005), One more step towards a warmer
 1010 Arctic. *Geophys. Res. Lett.* 32, L17605, doi: 10.1029/2005GL023740.
 1011 Rae, J.G.L., H.T. Hewitt, A.B. Keen, J.K. Ridley, J.M. Edwards, and C.M. Harris (2014), A
 1012 sensitivity study of the sea ice simulation in HadGEM3, *Ocean Model.* 74, 60–76,
 1013 doi:10.1016/j.ocemod.2013.12.003.
 1014 Ricker, R., S. Hendricks, F. Girard-Ardhuin, L. Kaleschke, C. Lique, X. Tian-Kunze, M.
 1015 Nicolaus, and T. Krumpfen (2017a), Satellite observed drop of Arctic sea ice growth in winter
 1016 2015-2015, *Geophys. Res. Lett.*, doi:10.1002/2016GL072244.
 1017 Ricker, R., S. Hendricks, L. Kaleschke, X. Tian-Kunze, J. King and C. Haas (2017b), A weekly
 1018 arctic sea-ice thickness data record from merged cryosat-2 and SMOS satellite data, *The*
 1019 *Cryosphere*, 1-27, doi:10.5194/tc-2017-4.
 1020 Ricker, R., S. Hendricks, V. Helm, H. Skourup, and M. Davidson (2014a), Sensitivity of
 1021 CryoSat-2 Arctic sea-ice freeboard and thickness on radar-waveform interpretation, *The*
 1022 *Cryosphere*, 8 (4), 1607-1622, doi:10.5194/tc-8-1607-2014.
 1023 Rigor, I.G., J.M. Wallace and R.L. Colony (2002), Response of sea ice to the Arctic Oscillation,
 1024 *J. Clim.*, doi:10.1175/1520-0442(2002)015<2648:ROSITT>2.0.CO;2.
 1025 Schröder D., D. L. Feltham, D. Flocco, M. Tsamados (2014), September Arctic sea-ice minimum
 1026 predicted by spring melt-pond fraction. *Nature Clim. Change*, doi 10.1038/NCLIMATE2203.
 1027 Screen, J.A and I. Simmonds (2010), The central role of diminishing sea ice in recent Arctic
 1028 temperature amplification, *Nature*, 464, 1334-1337.
 1029 Serreze, M.C., A.P. Barrett, J.C. Stroeve, D.M. Kindig, M.M. Holland (2009), The emergence of
 1030 surface-based Arctic amplification, *The Cryosphere*, 3, pp. 11–19.
 1031 Stroeve, J. and D. Notz (2015), Insights on past and future sea-ice evolution from combining
 1032 observations and models, *Global and Planetary Change*, doi:10.1016/gloplacha.2015.10.011.
 1033 Stroeve, J.C., T. Markus, L. Boisvert, J. Miller and A. Barrett (2014), Changes in Arctic Melt
 1034 Season and Implications for Sea Ice Loss. *Geophysical Research Letters*,
 1035 doi:10.1002/2013GL058951.
 1036 Stroeve, J.C., M.C. Serreze, J.E. Kay, M.M. Holland, W.N. Meier and A.P. Barrett, (2012). The
 1037 Arctic’s rapidly shrinking sea ice cover: A research synthesis, *Clim. Change*, doi:
 1038 10.1007/s10584-011-0101-1.
 1039 Tilling, R. L., A. Ridout, A. Shepherd, and D. J. Wingham (2015), Increased arctic sea ice
 1040 volume after anomalously low melting in 2013, *Nature Geoscience*, 8 (8), 643–646.
 1041 Tilling, R. L., A. Ridout and A. Shepherd (2016), Tilling, R. L., A. Ridout, and A. Shepherd,
 1042 Near-real-time Arctic sea ice thickness and volume from CryoSat-2, *The Cryosphere*, 10,

Formatted: Font:Font color: Auto, Pattern: Clear

Formatted: Right: 0.25"

1043 doi:10.5194/tc-10-2003-2016.
1044 Tilling, R.L., A. Ridout, and A. Shepherd (2017), Estimating Arctic sea ice thickness and volume
1045 using CryoSat-2 radar altimeter data, *Advances in Space Research*,
1046 doi:10.1016/j.asr.2017.10.051.
1047 Tsamados M., D. L. Feltham, D. Schröder, D. Flocco, S. Farrell, N. Kurtz, S.Laxon, and S.
1048 Bacon (2014), Impact of variable atmospheric and oceanic form drag on simulations of Arctic
1049 sea ice. *J. Phys. Oceanogr.* 44 (1329-1353), doi:10.1175/JPO-D-13-0215.1.
1050 Tsamados, M., D. Feltham, A. Petty, D. Schröder and D. Flocco (2015), Processes controlling
1051 surface, bottom and lateral melt of Arctic sea ice in a state of the art sea ice model, *Phil.*
1052 *Trans. R. Soc. A* 373.2052, doi:10.1098/rsta.2014.0167.
1053 Warren, S.G., I.G. Rigor, N. Untersteiner, V.F. Radionov, N.N. Bryazgin, Y.I. Aleksandrov and
1054 R. Barry (1999), Snow depth on Arctic sea ice, *J. Clim.*, 12, 1814-1829.
1055 Willatt, R., S. Laxon, K. Giles, R. Cullen, C. Haas, and V. Helm (2011), Ku-band radar
1056 penetration into snow cover Arctic sea ice using airborne data, *Ann. Glaciol.*, **52**(57), 197–
1057 205.
1058
1059
1060
1061

Formatted: Right: 0.25"

1062
1063

Table 1. Regional trends in freeze-up, 2017 freeze-up date and anomaly (relative to 1981-2010 mean). Freeze-up is computed following Markus et al. (2009).

Region	Freeze-up Trend (days per decade)	2017 Mean Freeze-up (day of year)	2017 Freeze-up Anomaly (days)
Sea of Okhotsk	9.1	304	0.8
Bering Sea	6.7	338	25.2
Hudson Bay	7.9	333	16.9
Baffin Bay	8.0	312	13.2
E. Greenland Sea	5.6	267	2.7
Barents Sea	13.6	347	60.3
Kara Sea	10.7	314	36.6
Laptev Sea	9.0	272	10.7
E. Siberian Sea	11.8	286	27.1
Chukchi Sea	14.1	314	31.0
Beaufort Sea	8.9	279	23.4
Canadian Archipelago	4.9	268	12.7
Central Arctic	3.1	255	16.8
Pan-Arctic	7.5	288	19.6

1064
1065
1066
1067
1068
1069

Table 2. Mean November ice thickness and anomaly with respect to the 2011-2017 mean (in parenthesis) from CS2 derived from CPOM, AWI and NASA. Spatial mean is over Arctic Basin, defined as the area for which CS-data were available continuously for all 7 winter periods November to April 2010/2011 to 2016/17. This region corresponds to all three regions shown in Figure 1(c).

	November SIT CS2 CPOM (cm)	November SIT CS2 AWI (cm)	November SIT CS2 NASA (cm)	November SIT CICE-free (cm)
2010	183 (-6)	208 (-8)	198 (-7)	206 (+6)
2011	157 (-32)	174 (-42)	170 (-35)	185 (-15)
2012	173 (-16)	192 (-24)	177 (-28)	152 (-48)
2013	212 (+23)	246 (+29)	243 (+38)	208 (+08)
2014	207 (+18)	239 (+23)	226 (+21)	231 (+31)
2015	196 (+7)	229 (+13)	217 (+12)	219 (+19)
2016	193 (+4)	225 (+9)	204 (-1)	199 (-1)
2010-2016 mean	189	216	205	200

1070
1071
1072
1073
1074
1075

Formatted: Normal, Don't keep with next

Formatted: Font:Not Bold, Italic, Font color: Auto

Formatted: Right: 0.25"

1076 **Table 3.** Mean April sea ice thickness (SIT) and anomaly with respect to the 2011-2017 mean (in
 1077 parenthesis) from three CS2 products (CPOM, AWI and NASA), and the CICE (free run 1985-
 1078 2017) and CICE runs initialized with CS2 ice thickness in November. The amount of
 1079 thermodynamic ice growth and dynamical ice change from the CICE model runs is also given.
 1080 Spatial mean is over Arctic Basin, defined as the area shown in Figure 1(d).

1081

	CryoSat-2 Results			CICE Simulations					
	April SIT CPOM (cm)	April SIT AWI (cm)	April SIT (NASA) (cm)	April SIT CICE free (cm)	April SIT CICE ini (cm)	Therm growth CICE free (cm)	Therm growth CICE ini (cm)	Dyn change CICE free (cm)	Dyn change CICE ini (cm)
1990-2017 Mean	n/a	n/a	n/a	283	n/a	107	n/a	-18	n/a
2010-2017 Mean	243	230	235	246	240	112	103	-15	-17
2011	239 (-4)	237 (+7)	227 (-8)	242 (-4)	241 (+1)	115 (+3)	104 (+1)	-18 (-3)	-20 (-3)
2012	235 (-8)	219 (-11)	218 (-17)	247 (+1)	233 (-7)	115 (+3)	110 (+7)	-9 (+6)	-12 (+5)
2013	230 (-13)	208 (-22)	210 (-25)	234 (-12)	237 (-3)	136 (+24)	117 (+14)	-16 (+1)	-19 (-2)
2014	261 (+18)	250 (+20)	254 (+19)	251 (+5)	249 (+9)	102 (-10)	94 (-9)	-12 (+3)	-17 (+0)
2015	264 (+21)	252 (+22)	254 (+19)	264 (+18)	255 (+11)	108 (-4)	103 (-0)	-18 (-3)	-22 (-5)
2016	239 (-4)	227 (-3)	228 (-7)	254 (+8)	241 (+1)	107 (-5)	101 (-2)	-15 (-0)	-17 (+0)
2017	230 (-13)	218 (-12)	238 (+3)	233 (-13)	227 (-13)	99 (-13)	92 (-11)	-14 (+1)	-13 (+4)

1082
1083

1084

1085

Formatted: Right: 0.25"

CICE simulations suggest the overall thinner ice in April 2017 is largely attributed to reduced thermodynamic ice growth. One would expect thermodynamic ice growth to be reduced in regions of enhanced snow depth and thicker November ice. Spatially, the largest reductions in thermodynamic ice growth during winter 2016/2017 occurred within the Chukchi Sea and north of the CAA and extending through the northern Beaufort Sea (on the order of -40 cm). These regions have very different explanations for reduced thermodynamic ice growth. Ice formed a month later than the 1981-2010 mean within the Chukchi Sea, reducing the number of days over which the ice could grow. In contrast, north of the CAA, winter ice growth was reduced in a region that showed positive November thickness anomalies, illustrating the strong dependence of thermodynamic ice growth on initial ice thickness. This region also had anomalously positive snow depths that extended through the northern Beaufort Sea, in agreement with extended regions of reduced thermodynamic ice growth.

While the CICE simulations show reduced thermodynamic ice growth for most of the Arctic over winter 2016/2017, ice growth was enhanced directly north of Utqiagvik, Alaska (formerly Barrow). However, this enhanced ice growth was offset by ice divergence, leading to overall thinner ice in the CICE simulations. In situ observations of level first-year ice thickness off the coast of Utqiagvik ranged between 1.35 and 1.40m during May (<http://arcus.org/sipn/sea-ice-outlook/2017/june>) and appear to be in better agreement with the CICE simulations, as well as the CPOM and AWI CS2 thickness estimates, while the NASA CS2 product shows positive thickness anomalies in that region. Positive thermodynamic ice growth anomalies are also found for a small region north of Greenland and within Fram Strait, as well as within some scattered coastal regions of the Chukchi, East Siberian, Laptev and Kara seas.